OCS Study
MMS 2005-039

Coastal Marine Institute

Aspects of the Louisiana Coastal Current

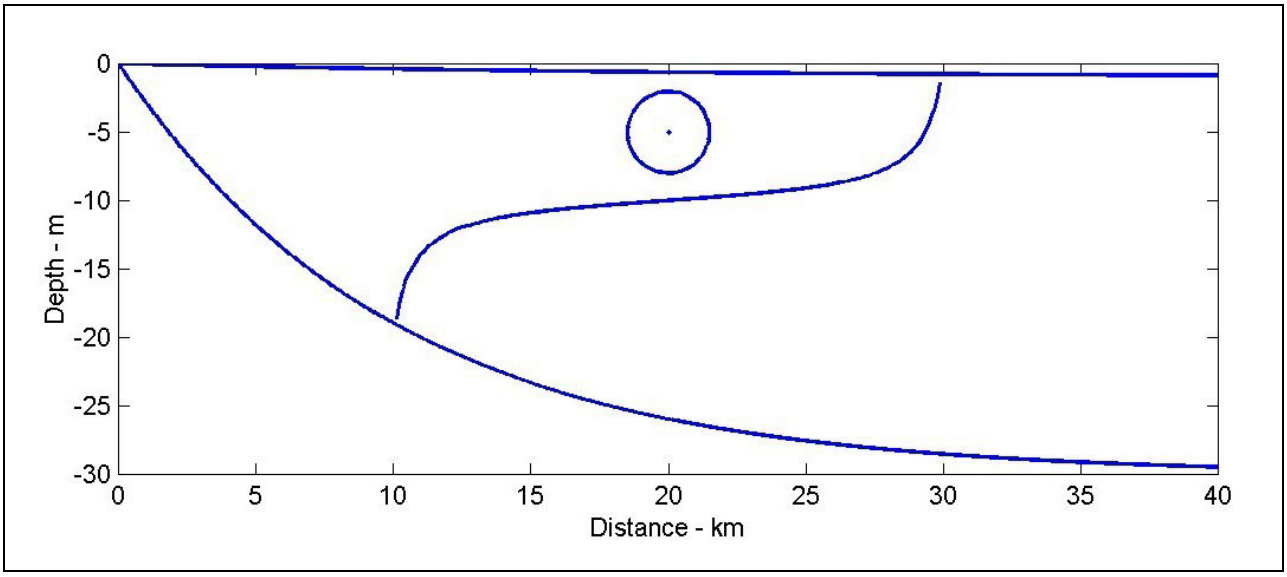

MMS U.S. Department of the Interior
Minerals Management Service
Gulf of Mexico OCS Region

LSU Cooperative Agreement
Coastal Marine Institute
Louisiana State University

OCS Study
MMS 2005-039

Coastal Marine Institute

Aspects of the Louisiana Coastal Current

Authors

Larry J. Rouse, Jr.
William J. Wiseman, Jr.
Masamichi Inoue

June 2005

Prepared under MMS Contract
14-35-0001-30660-19936
by
Coastal Marine Institute
Louisiana State University
Baton Rouge, Louisiana 70803

Published by

U.S. Department of the Interior
Minerals Management Service
Gulf of Mexico OCS Region

Cooperative Agreement
Coastal Marine Institute
Louisiana State University

DISCLAIMER

This report was prepared under contract between the Minerals Management Service (MMS) and Louisiana State University. This report has been technically reviewed by the MMS and approved for publication. Approval does not signify that the contents necessarily reflect the view and policies of the Service nor does mention of trade names or commercial products constitute endorsement or recommendation for use. It is, however, exempt from review and compliance with MMS editorial standards.

REPORT AVAILABILITY

Extra copies of the report may be obtained from the Public Information Office (MS 5034) at the following address:

U.S. Department of the Interior
Minerals Management Service
Public Information Office (MS 5034)
Gulf of Mexico OCS Region
1201 Elmwood Park Boulevard
New Orleans, Louisiana 70123-2394

Telephone Number: (504) 736-2519
1-800-200-GULF

CITATION

Suggested Citation:

Rouse, L. J., Jr, W. J. Wiseman, Jr., and M. Inoue. 2005. Aspects of the Louisiana Coastal Current. U.S. Dept. of the Interior, Minerals Management Service, Gulf of Mexico OCS Region, New Orleans, LA. OCS Study MMS 2005-039. 50 pp.

ABOUT THE COVER

The cover art shows a schematic diagram of the westward (downcoast) flowing Louisiana Coastal Current (LCC). The sea surface tilts up towards the coast. The low salinity waters of the LCC are separated from the higher salinity mid-shelf waters by a strong bottom-to-surface frontal boundary. The westward current is indicated by the circle with a dot inside (an arrowhead coming out of the page).

TABLE OF CONTENTS

LIST OF FIGURES

LIST OF TABLES

I. INTRODUCTION

1.1 Morphology of the Northwestern Gulf of Mexico Shelf

In the following, we will define the northwestern Gulf of Mexico shelf as originating at the birdfoot or Belize delta of the Mississippi River and extending westward to the Mexican border (Figure 1). The shelf is extremely narrow near the birdfoot delta and broadens dramatically to the west. Immediately west of the delta, the shelf is cut by the Mississippi Canyon. There are indications in some data sets that the presence of this canyon influences the local circulation and allows cross shelf transport of waters with deepwater characteristics (A. E. Jochens, personal communication). Offshore of the Texas-Louisiana border the shelf attains its maximum width of approximately 191 km. Further west, it narrows considerably. At approximately 96^{o} W, the shelf begins to turn to a north-south orientation as it continues to narrow. The shelf width at the Texas-Mexican border is only 76 km.

Assuming the shelf break lies at approximately 100 m, the mean cross shelf slope varies from 0.008 near the Mississippi delta to .0005 offshore of the Texas-Louisiana border to 0.001 near the Mexican border. The slope, though is not uniform. Nearshore, the bottom topography is concave upwards. Despite the relatively smooth character of the shelf, there are a number of shoals over the inner shelf such as Ship Shoals near 91^{o} W, Trinity Shoal near 92.25^{o} W, and the Sabine Bank near the Texas-Louisiana border. There is a break in bottom slope at mid-shelf over the broadest regions of the shelf. The offshore slope is steeper than that over the inner portions of the shelf. This feature is important for the formation of dense water over the mid-shelf during some winters (Nowlin and Parker, 1974), but is of little importance to the dynamics of the inner shelf and the Louisiana Coastal Current.

1.2 River Discharge

The Mississippi River discharge to the northwestern Gulf of Mexico shelf is the dominant source of fresh water to the region (Cochrane and Kelly, 1986; Dinnel and Wiseman, 1986). The Mississippi River system drains 41% of the contiguous United States and parts of two Canadian provinces. It discharges 94% of the fresh water emptied onto the northwestern Gulf of Mexico shelf (Cochrane and Kelly, 1986). Natural processes cause the river to change the location of its major delta lobe approximately every 1000 years. The birdfoot delta has been dominant since European settlement, but the river is seeking a more efficient route to the sea through the Atchafalaya delta, which enters into Atchafalaya Bay. The US Corps of Engineers has been tasked with maintaining 70% of the river system's flow through the birdfoot delta.

The annual (1979-2002) discharge of the system is 692 km^3 (Figure 2). This discharge has a strong seasonal signal (Figure 3). Maximum discharge is associated with snowmelt in the upper portions of the drainage basin. Interannual variability is strong. Due to the integrating effect of the large drainage basin, the ratio of maximum to minimum discharge during a year is significantly less than observed in smaller systems. Long-term discharge data from Tarbert Landing just north of Baton Rouge, but below the Old River control structure, were obtained. A

seasonal Kendall-tau test for trends (Hirsch et al., 1982) indicated that discharge has increased significantly (α=0.05) over the length of the record (1930-2002) in the later months of the year. When the record is shortened to include the period since 1979, when the ratio of Mississippi River to Atchafalaya River discharge was stabilized at its mandated ratio, only the month of September indicated a significant trend in discharge and this trend is negative!

1.3 Winds

Winds in the region are significantly influenced by the Bermuda high pressure system. When the system is strong and in a southwesterly location, typical of summer conditions, the northwestern Gulf of Mexico shelves are subject to breezes from the south and southeast. The only persistent strong winds are associated with the occasional tropical storm or hurricane. When the high pressure system retreats to the northeast during winter, the dominant synoptic weather pattern is the cold air outbreak (DiMego et al., 1976). These recur with time scales of 3 to 10 days. Preceding the frontal passage, strong winds blow from the south. Following the front, intense winds blow cold, dry air off the continent. During frontal passage, wind stress changes direction by 180 degrees (Dinnel, 1988), wind-driven currents may intensify and change direction (Crout et al., 1984; Wiseman and Kelly, 1994), and latent air-sea heat flux increases significantly (Nowlin and Parker, 1974; Huh et al., 1984).

Because of subtle changes in the coastal orientation, subtle changes in wind stress direction may have significant effects on currents as the winds change from downwelling to upwelling favorable (Cochrane and Kelly, 1986; Howard, 1996). Gutierrez de Velasco and Winant (1996) describe the larger, low-passed wind patterns for the entire Gulf of Mexico for the three-year period 1991-1993 with a focus on the seasonal and annual means. Howard (1996) discusses the monthly mean stress distribution for the LATEX period (1992-1994) with emphasis on the spring transition from downwelling favorable to upwelling favorable conditions. Wiseman et al. (1998) stress the importance of seasonal and interannual variability in the wind stress distribution over the region. An example of this variability is presented in the plots of wind pseudo-stress variance ellipse characteristics presented in Figure 4.

1.4 Louisiana Coastal Current

In response to the massive freshwater discharge of the Mississippi River system and the predominantly downwelling favorable winds of the northwestern Gulf of Mexico shelf, a strongly stratified coastal current, known as the Louisiana Coastal Current (Wiseman and Kelly, 1994), flows westward along the Louisiana inner shelf. During much of the year, this flow extends into Texas waters and even onto the Mexican shelf (Cochrane and Kelly, 1986). Seasonal cycles of both the stratification (Wiseman et al., 1997) and currents (Nowlin et al., 1998) are observed to occur in response to similar cycles in the river discharge and winds.

The seasonal cycle of stratification within the Louisiana Coastal Current between the Mississippi and Atchafalaya River deltas was described from eight years of occasional CTD casts at a site in 20 m of water by Wiseman et al. (1997). Although the buoyancy flux associated with fresh

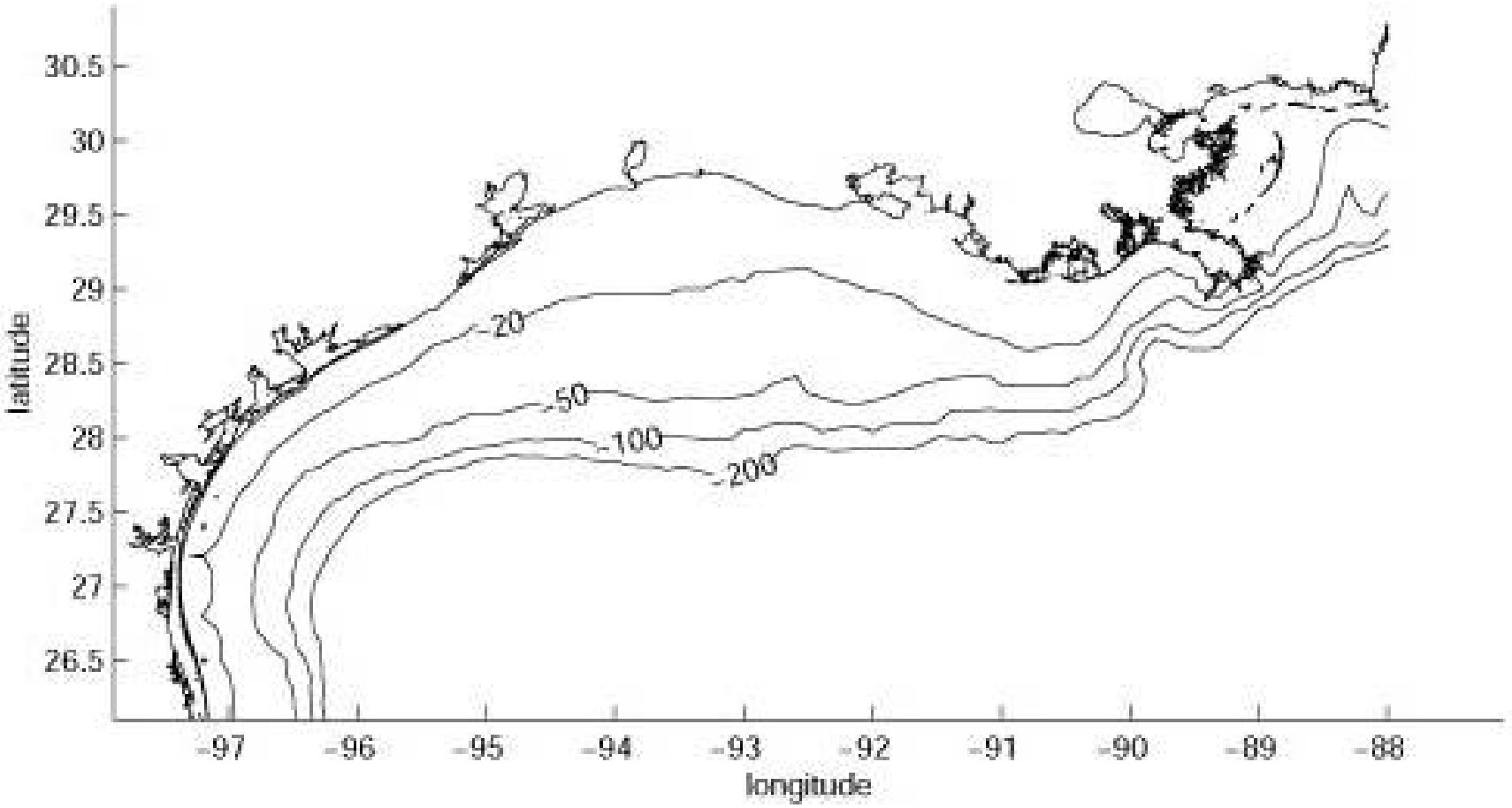

Figure 1. Northwestern Gulf of Mexico shoreline and bathymetry interpolated to 0.1 degree from DBDB5 data.

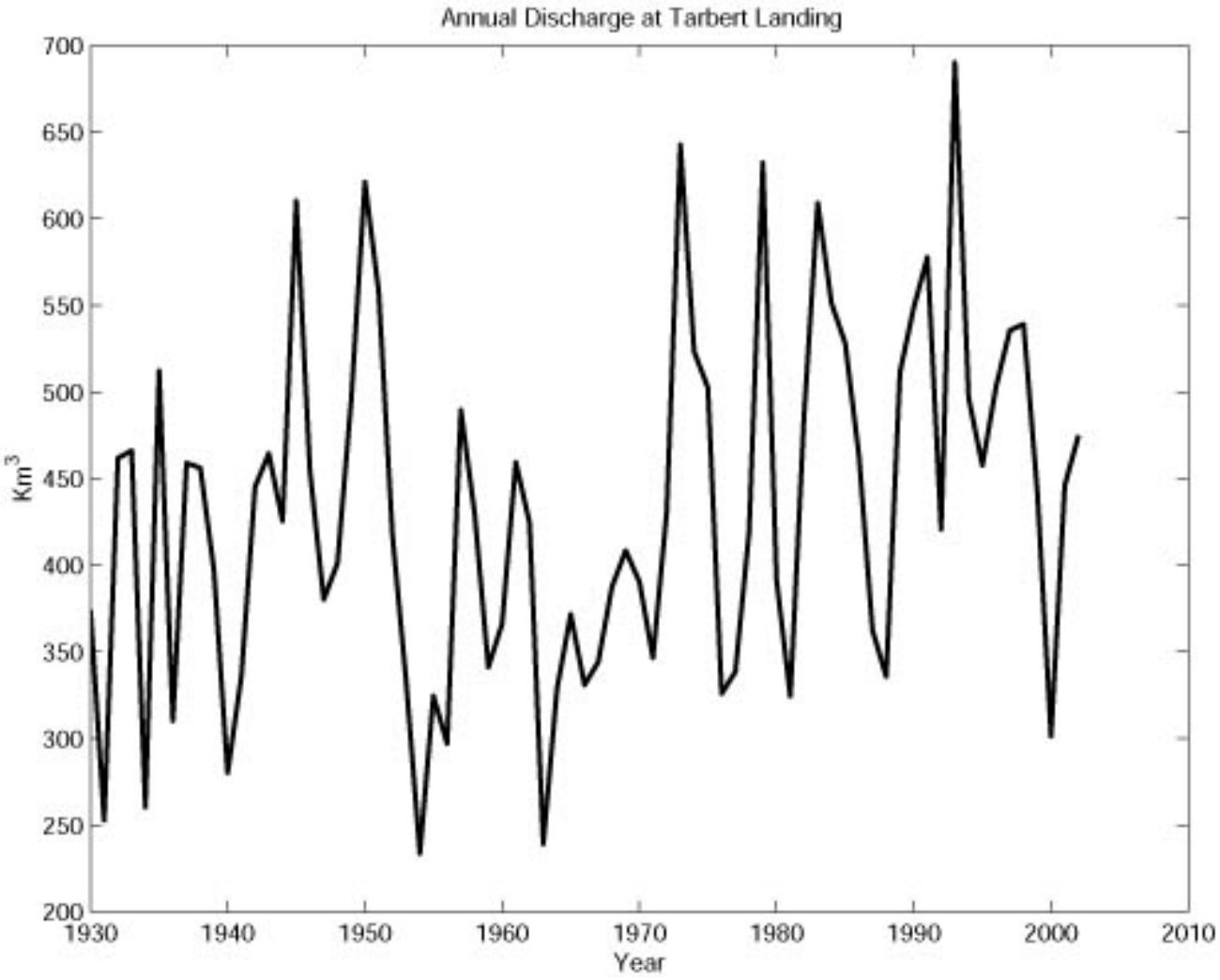

Figure 2. Annual discharge of the Mississippi River as measured at Tarbert Landing.

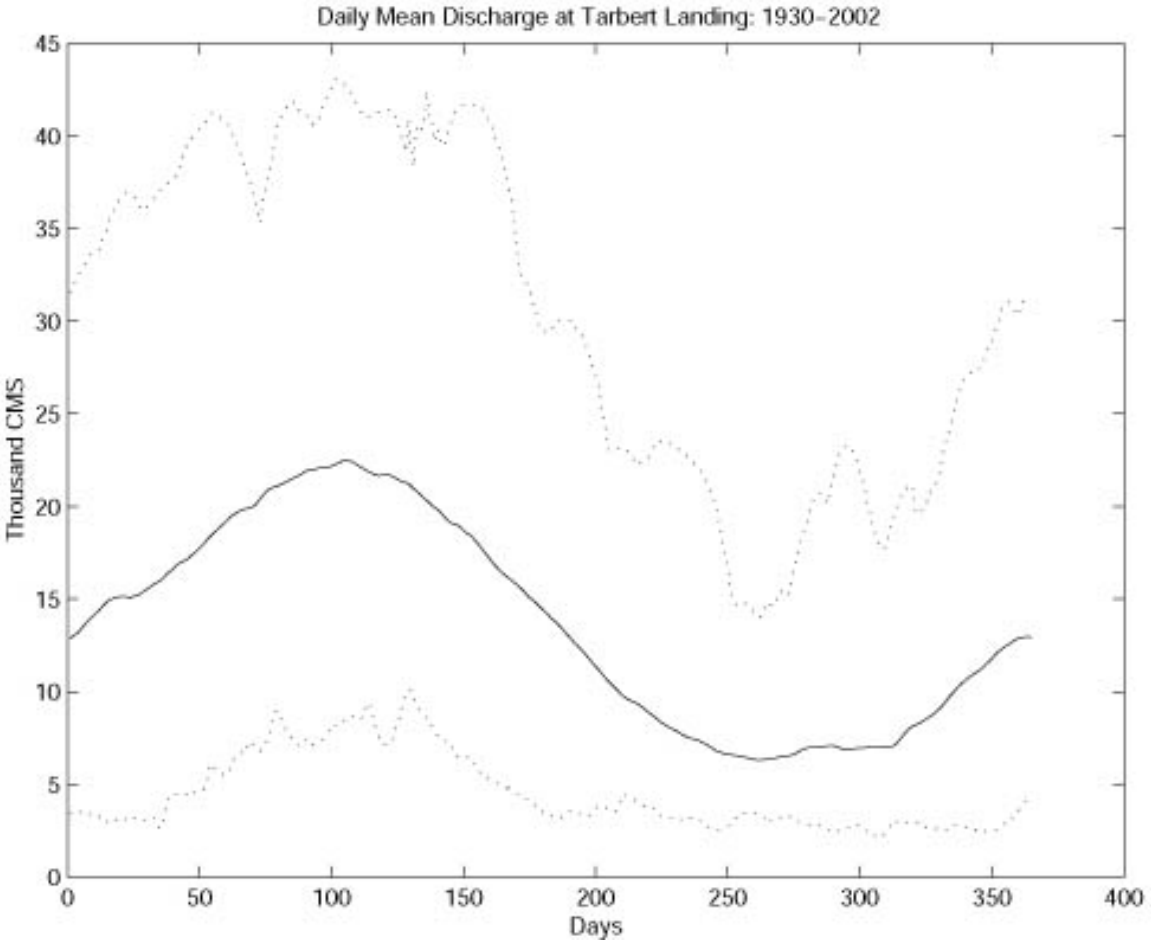

Figure 3. Long-term daily mean Mississippi River discharge (solid) at Tarbert Landing with maximum and minimum observed discharge (dotted).

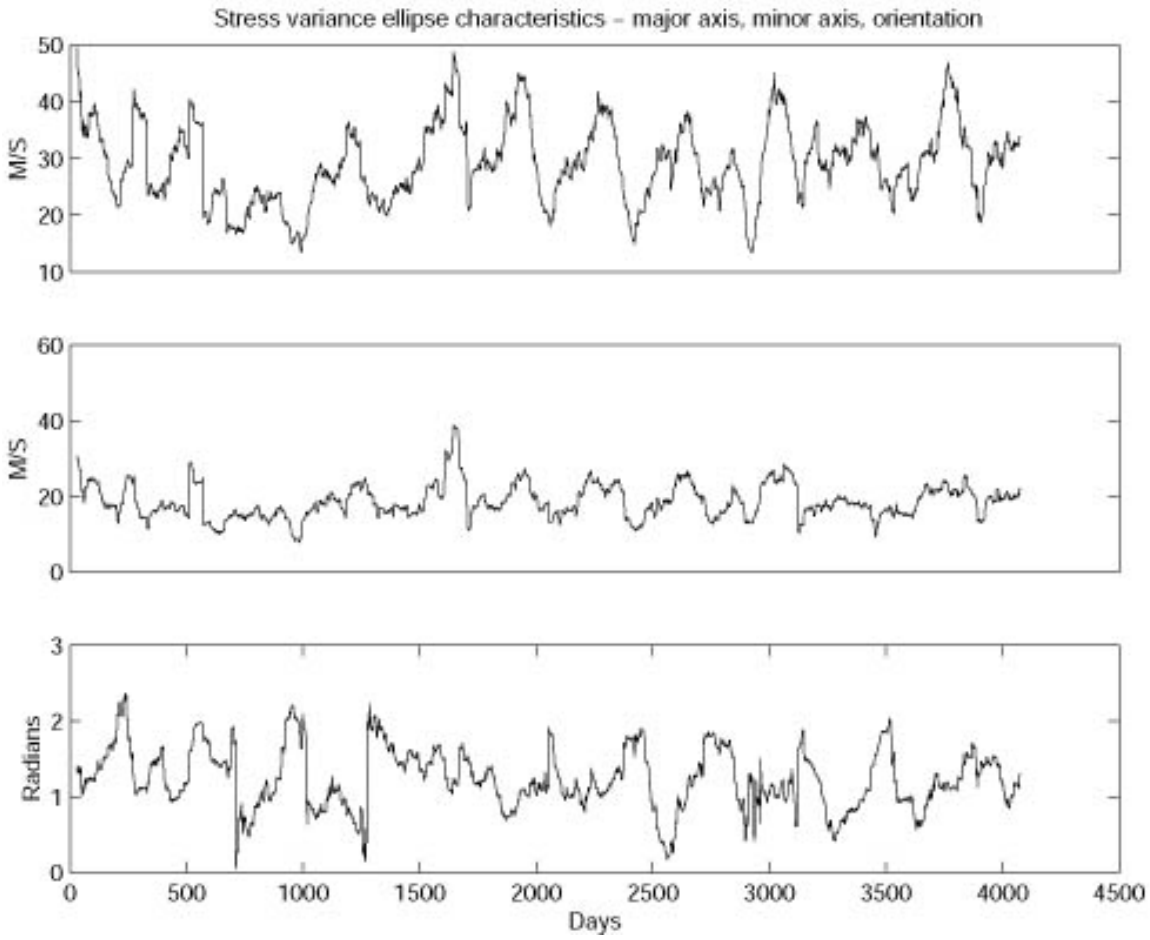

Figure 4. A 10-year record of the major (top) and minor (middle) axes of the wind-stress variance ellipse from a station along the Texas coast. Parameters are computed over a 60-day window. The orientation of the ellipse is also shown (bottom). (Wiseman et al., 1998)

water from the river system represents the dominant control on stratification, vernal and summer solar heating are not without influence. On a classical temperature and salinity diagram, the path of surface water mass characteristics for surface and bottom waters rotate in contrasting directions. The surface waters are cold and saline at the onset of the year. In response to the spring flood and increasing length of day, the waters heat and freshen through the spring months. After the spring flood ends, salinity drops gradually, but the waters continue to increase in temperature. By late summer/early fall, they begin to cool dramatically, while continuing to increase slowly in salinity. The bottom waters increase in salinity throughout the spring and summer months as the halocline precludes freshening through mixing with the overlying waters and weak vertical entrainment of lower layer waters into the upper layers results in a hypothesized weak replacement flow from offshore. Throughout the fall and early winter, the bottom waters cool dramatically and freshen as the halocline begins to weaken. This counter-rotation of water mass characteristics on the T-S diagram reflects increasing density stratification

throughout the first half of the year and decreasing stratification in the latter part of the year. Data at 7 and 20 m depth from a recent mooring at the same location as this station data confirm this picture of a seasonal pattern of stratification, but also indicate the importance of high-frequency perturbation of the stratification by wind-driven mixing (Wiseman et al., 2004).

Current understanding of the dynamics of this region remains less than satisfactory. Winter flow regimes are highly frictional. The dominant time scales of the sub-tidal currents are associated with the synoptic weather band (3 - 10 days). Currents are highly coherent with wind stress (Crout et al., 1984) and the currents are coherent both vertically and horizontally (F. J. Kelly, personal communication). As stratification increases, coherence of near-bottom currents with the local winds may decrease, e.g. Chuang and Wiseman (1983). Recent observations confirm these results. During summer, near-bottom flows may oppose the near-surface flows or stagnate (Crout, 1983). It is not yet clear whether results observed west of the Atchafalaya Delta, where the Louisiana Coastal Current flows over somewhat shallower water, are directly comparable to flows between the Mississippi and Atchafalaya Deltas, since the initial discharge plume of the latter rapidly detaches from the bottom while that of the former is bottom attached. Seasonal changes in very low-frequency flow in direct response to changes in the local wind have been noted for many years (Cochrane and Kelly, 1986). Cho et al. (1998) confirm these results, but stress the interannual variability of flows. A recent eight-month record from an ADCP in 20 meters of water at 91.25^{o} W suggests a mean circulation consistent with downwelling flow. Variability about this pattern, though, is significant. The dominant EOF, accounting for 82% of the sub-inertial flow variance, is barotropic and moderately sheared. The second EOF mode, which is consistent with a two-layered system, accounts for only 13% of the variance. Flows consistent with upwelling and downwelling are frequent in the subinertial cross shelf current structure.

The frequency band over which wind forcing is important overlaps that where quasi-geostrophic dynamics may be expected to contribute significantly to the transport. It is unclear, with existing data sets, how one might determine the importance of geostrophic dynamics in this region. As a first attempt to accomplish this, ten-day low-pass filtered current shear data in 10 m of water were compared with local thermal wind shear. The results exhibited an approximately one-to-one linear fit of one data set to the other, suggesting a nearly geostrophically balanced shear in these shallow, but highly stratified, waters.

1.5 Historical Investigations

Some of the earliest concerted efforts devoted to understanding the circulation and stratification of the Texas-Louisiana shelf were Lagrangian (Kimsey and Temple, 1963, 1964; Hill et al., 1975; Schideler, 1979). These, though, were rapidly followed by a series of Eulerian studies that were reported in the gray literature (Oetking et al., 1973; Armstrong, 1976; Gosselink et al., 1976; Angelovic, 1977; Gunn, 1978; Frey, 1981; Hann and Randall, 1981; Nowlin et al., 1998). The data collected during these studies often was reanalyzed for publication in the refereed literature and was supplemented by other small-scale efforts. These efforts focussed on two aspects of the Louisiana Coastal Current: stratification and velocity structure.

The seminal work by Cochrane and Kelly (1986) synthesized existing knowledge of the Louisiana-Texas shelf. This effort was based largely on observed temperature and salinity characteristics of the water, but also included the isolated observations of flow and existing climatologies of coastal wind fields. They defined a seasonal cycle of near-surface circulation that remains essentially unchanged today. The shelf circulation was seen to be dominated by a cyclonic circulation cell, driven by Mississippi and Atchafalaya River discharge and downwelling favorable winds, during most of the year. A nearshore reversal of flow, in response to upwelling favorable winds along the Mexican and south Texas shelves occurred from late spring to summer and extended into Louisiana waters during mid-summer. Recent observations confirm this pattern, although they stress the interannual variability associated with it (Nowlin et al., 1998). Dinnel and Wiseman (1986) elaborated on the distribution of Mississippi River water over the shelf and its seasonal and interannual variability. The question of the cross shelf dispersion of this water, though, remained open. Wiseman et al. (1982) described the seasonal and spatial distribution of water properties within the plume of the Mississippi River delta, while Wiseman et al. (1975) focussed attention on the fine-structure in the water column in the same region.

Working alone, Ned Smith produced some of the first publications describing the nearshore flows along the Texas inner shelf (Smith, 1975, 1978). These strongly influenced Cochrane and Kelly as they developed their synthesis of the shelf circulation. Later, much of the historical data, originally confined to the gray literature, was reanalyzed and published in the open literature. Crout et al. (1984) described the relationship of inner shelf currents, during the energetic winter season, to the local winds and found strong evidence that a simple local linear model would describe much of the observed variability. Wiseman and Kelly (1994) described the changes in flow structure across the inner shelf and the response of the flow field to the spring flood of the Mississippi River system. Daddio et al. (1978) were the first to focus attention on the strong inertial oscillations over the inner shelf in response to cold air outbreaks in the presence of strong stratification.

More recent studies have used extensive data sets collected with modern instrumentation to describe the flow and stratification variability near the Mississippi River delta (Hitchcock et al., 1997; Wiseman et al., 1997; Wiseman et al., 2004). Downcoast of the Atchafalaya River delta, data from the LATEX program (Nowlin et al., 1998) have been analyzed and reported on extensively, e.g. Cho et al. (1998); DiMarco and Reid (1998); Li et al. (1997). Finally, Dinnel et al. (1997) performed a seasonal analysis of the low-order seasonal statistics of available upper layer current observations from the inner shelf from south Texas to the Florida panhandle, documenting the spatial variability of these characteristics.

1.6 Summary

From the abbreviated preceding paragraphs, it should be clear that much information and extensive data sets are available from the Louisiana-Texas inner shelf region. These data, while incomplete and occasionally misleading, provide a vast source of information for model development, model forcing, and model verification. In the next chapter, we briefly review the level of success achieved by existing models of the region. It will become clear that existing

models of the region have had some limited success in hindcasting observations, but that issues remain with all of these. In light of this, it may be of interest to investigate how successful simple local models are in hindcasting observations. Thus, we follow the review of existing models with application of simple concepts to the Louisiana Coastal Current. In Chapter III, we investigate the ability of a vertically-integrated model forced by low-frequency winds to explain the observed current fields at frequencies below the weather band. Yankovsky and Chapman's model of a coastal current controlled by bottom boundary layer processes is compared to observations in Chapter IV. We discuss the potential role of pressure gradients in Chapter V. Finally, we summarize and critique these results, in Chapter VI, and offer suggestions for fruitful areas of future progress.

II. OVERVIEW OF EXISTING MODELS

2.1 Introduction

The noted statistician George P. E. Box once stated "All models are wrong-but some models are useful". It would be easy to ignore, refute, or criticize historical modeling efforts over the LATEX inner shelf. A more useful approach might be to consider the assumptions and goals of the models, to determine their success at achieving their stated goals, and to assess the degree to which their lack of success is attributable to their assumptions. It is only recently that long simultaneous records from multiple sites have become available for comparison to model output. Necessarily, therefore, early models focused on short time scales, usually subinertial, and specific sites and seasons when stratification clearly was either a dominant or second-order concern. Approaches to modeling have generally involved a numerical solution to equations that often were of reduced dimensionality.

2.2 One-dimensional Models

While the focus of this chapter is on subinertial motions, it should be mentioned that the strong stratification and the impulsive wind forcing found over the Louisiana-Texas shelf result in the generation and persistence of energetic inertial oscillations. These were first noted and modeled by Daddio et al. (1978), following the approach of Pollard and Millard (1970), and later by Chen et al. (1996). A full understanding of the dynamics of these currents across the breadth of the shelf remains an open topic of investigation.

Much of the one-dimensional modeling of the currents on the Louisiana-Texas shelf is based on the early observations of strong coherence between local wind and currents, e.g. Crout et al. (1984). These observations suggested that a local linear balance between wind stress and bottom stress could explain the measured flows within the weather band. Following Scott and Csanady (1976), Crout (1983) attempted to estimate the intensity of an alongshore pressure gradient term in an expanded model that included wind stress, bottom stress, and alongshore pressure gradients. (This will be discussed further in Chapter V.) Murray (1998) and Walker et al. (2001) were moderately successful in describing observed currents, for brief periods of time, with a similar model that supplemented the wind stress/bottom stress balance with a local acceleration term.

Chuang and Wiseman (1983) considered the linearized, vertically-integrated equations of motion and continuity. They assumed alongshore homogeneity and forcing by an oscillatory wind stress. Bottom topography was allowed to vary in the cross-shore direction. Thus, the equations to be solved were

$$\partial U/\partial t - fV = -gh\partial\zeta/\partial x + \tau_x - rU/h \quad (1)$$

$$\partial V/\partial t + fU = \tau_y - rV/h \quad (2)$$

$$\partial U/\partial x = -\partial \zeta/\partial t \quad (3)$$

with boundary conditions

$$U = 0 \text{ at } x = 0 \text{ (the coast)} \quad (4)$$

$$\zeta = 0 \text{ as } x \rightarrow \infty \quad (5)$$

where U and V are the transports in the alongshore (x) and cross-shore (y) directions, f is the Coriolis parameter, h is the water depth, τ_x and τ_y are the wind stress components in the x and y directions, respectively, r is a linear drag coefficient, ζ is the sea level elevation and t is time. Assuming a wind stress that varies as $e^{i\sigma t}$, taking the Fourier transform of the governing equations, and eliminating U and V, one obtains a second order differential equation for ζ, which can be solved numerically. The solution, assuming a realistic cross-shore bottom profile, indicated insensitivity to the frequency of cross-shore wind forcing, but a sensitive dependence upon the water depth at the coast; sea level set-up being higher for shallower nearshore waters. These results compared well with observations from five-month records during the winter of 1962-1963 at Galveston, TX and Eugene Island, LA. Similarly, the strong, frequency-dependent response of sea level to an oscillatory alongshore wind stress at Galveston suggested a drag coefficient equal to 0.01 cm/s. The relative insensitivity of the sea level response to forcing frequency at Eugene Island indicated a much larger drag coefficient, near 0.1 cm/s, at this site.

Chuang and Wiseman argue that the increased drag coefficient appropriate to the solution at Eugene Island may be due to wave-current interactions during intense cold air outbreaks. Nevertheless, they suggest that this explanation is not sufficient to account for the abnormally large coefficient required to fit the model solution to observations. An alternative explanation is that some other important process is missing from the model formulation. It has been suggested that alongshore pressure gradients of small spatial scale may be the source of the mismatch. Another possibility is the absence of an appropriate lateral mixing scheme in the model. Finally, the assumption of alongshore homogeneity was made for mathematical convenience rather than being justified from physical arguments.

The models of Chuang and Wiseman (1983), Murray (1998) and Walker et al. (2001), as well as the statistical analyses of Crout et al. (1984), discussed thus far have assumed non-stratified flow and focused on vertically-integrated transport rather than on the sheared flow expected in a real system. This assumption was common both for mathematical convenience and because there were few data sets available for model verification that resolved the vertical structure of the flow field. Nevertheless, the importance of stratification was clearly recognized (see Chapter I). As more and better data sets became available, including more than a single current meter in the vertical, the possibility of verifying models that included vertical structure became a reality. The first such model for this region was that of Lewis and Reid (1985). They solved the normal mode equations (Veronis and Stommel, 1956) for a linearized, two-layered system given oscillatory wind stress forcing and assuming alongshore homogeneity. They were quite successful in hindcasting the autumn and winter energy levels in both the surface and lower layers, but underpredict the energies across the weather band during the summer months. They note that their normal mode approach implies that their baroclinic friction represents energy loss

from both layers as a function of vertical shear rather than energy transfer between layers – a more typical interpretation. The underprediction of summer energy levels is attributed to shelf wave phenomena. Evidence of propagating shelf waves over the Texas-Louisiana shelf is sparse. The model by Current (1996), to be discussed below, is based on the assumed existence of such waves. Unpublished data sets (E. Jarosz, personal communication; J. She, personal communication) suggest the existence of such waves, but the results are only marginally significant in a statistical sense. Again, the reduced dimensionality of the model and missing physics may be the culprit, as was suggested for the Chuang and Wiseman model. Alongshore pressure gradients are still missing from the model, lateral mixing processes are absent, and vertical mixing and dissipation is highly idealized.

2.3 Two-dimensional Models

Building on the success of the previous modeling efforts and the assumption that shelf wave motion may account for a portion of the mismatch between observations and model hindcasts, Current (1996) developed a spectral shelf wave model of the Texas-Louisiana shelf that could be verified using the extensive data sets from LATEX-A (Nowlin et al., 1998). Current assumes a quasi-linear, viscous conservation of horizontal momentum, locally hydrostatic pressure, and three-dimensional non-divergence of the velocity field. A bottom slip condition and a rigid lid are imposed. The upstream boundary condition is data driven, while a radiation boundary condition is imposed at the downstream boundary. The effects of the seasonally-varying density structure are imposed and the derived equations ultimately are solved for the volume transport on a boundary fitted coordinate system. The dissipative terms in the equations depend upon a careful evaluation of the bottom stress. A non-linear formulation of this term was carefully derived to yield results that were significantly improved over those obtained with a linear bottom friction coefficient.

The model was verified by comparing 40-hr low-passed current and water level observations from the shelf with the subinertial response of the tuned model. The average r-squared value between the hindcast and observed currents over the inner shelf (depths less than 50 m) was 0.46, but at individual meters the model explained nearly two-thirds of the variance observed. The comparisons were generally best at the inshore meters. When the comparisons are made on a monthly basis, it is interesting to note that the comparison was worst during the months of July and August, similar to the results of Lewis and Reid (1985), when the dynamics of the inner shelf are different from those prevalent during non-summer months. Alternatively, the explanation could lie in a degraded forcing field as many of the LATEX meteorological sensors were removed during the hurricane season for protection (S. A. Hsu, personal communication). Comparisons of simulated and observed water levels proved even superior to the current comparisons. Mean r-squared values were 0.55.

Chen et al. (1997) used a two-dimensional version of the Princeton Ocean Model (Blumberg and Mellor, 1987), overlain with a simple NPZ model of the biological dynamics, to study the physical-biological coupling offshore of the Atchafalaya River delta. The model was structured as a vertical slice across the shelf with longshore homogeneous conditions. The onshore boundary conditions allowed for a specified mass flux per unit longshore distance from the river.

The offshore boundary condition was a radiation condition applied at the edge of a sponge layer. A free surface was specified to allow for tidal forcing from the open basin. A Mellor-Yamada level 2.5 turbulence closure scheme was used. When run with river flow parameters characteristic of spring 1993 and no wind forcing, the model was able to reproduce the observed nutrient and phytoplankton distributions inshore of the haline front that separates the low salinity inshore waters from saltier midshelf waters. This suggests that the dominant physics affecting the biology were adequately reproduced by the model, including the cross-shelf circulation and stratification. The alongshore flow after 30 days of model run was significantly higher than observed in the region studied (Nowlin et al., 1998; Dinnel et al., 1997). The reasons for the accelerated current are unclear. Longshore pressure gradients are absent from the model. Their influence cannot be estimated. The bottom topography used in the model is deeper than the observed bathymetry, thus frictional dissipation of the highly stratified flows may be too weak. Finally, the Mellor-Yamada turbulence closure scheme may be inappropriate for such highly stratified situations (Garvine, 2001).

2.4 Fully Three-dimensional Model

A fully three-dimensional version of the Princeton Ocean Model (Blumberg and Mellor, 1987) was implemented on a curvilinear grid covering the entire Gulf of Mexico, the northern Caribbean Sea, and parts of the Atlantic Ocean (Herring et al., 1999). The grid had maximum resolution over the northwestern shelf of the Gulf of Mexico. The model assumed a fixed horizontal eddy viscosity for most of the domain, but used a Smagorinsky (1963) closure scheme over the shelf. River inflow from 34 rivers was specified using real data. Evaporation was assumed to balance precipitation and surface heat flux was imposed from climatology. The model output was compared with current meter and water level data, as well as salinity data (Wiseman et al., 2000). This latter data was believed to represent an integrated response to the time-varying flows over the shelf. The mean flows for the 33-month data set available compared well. Flow means were of essentially the same magnitude and the same direction in all but a few sites. The r-squared values of the comparison between complex observed and hindcast current vectors generally ranged from 0.36 to 0.5. When only the alongshore components were considered, the r-squared values increased to values approaching those obtained by Current (1996). (It should be remembered that Current's analysis imposed an upstream boundary condition derived from current observations, while the present model used only wind stress and river flow as input. When the shelf wave model domain was extended to the Mississippi Delta and forced by wind only, the r-squared values dropped slightly at the upstream moorings, reducing the overall r-squared values slightly as well - C. Current, personal communication.) The phase of the complex correlation coefficient between observations and hindcast currents was near zero. Coherence-squared between the observed and hindcast currents of Herring et al. (1999) was only significant at the very lowest frequencies resolved. Visual comparison of the records suggest that the two signals exhibit periods of excellent correlation interspersed with periods of much poorer correlation. This may be due to the quality of the wind stress field used to force the model (Wiseman et al., 2000). Furthermore, there were indications in the data that momentum did not mix downward sufficiently rapidly in the model, suggesting issues with the turbulence closure scheme that needed further work. Comparisons did not improve when the grid size was halved. Thus, grid resolution does not appear to be the dominant cause of the

model-data discrepancies of the Herring et al. (1999) three-dimensional modeling study.

Comparison with the water levels was better than for the currents, as is to be expected. The salinity fields hindcast by the model did not differ significantly from the observations at the 95% level. Nevertheless, there were consistent patterns in the error signal that should be remedied. The surface salinities were, on average, saltier than the observations and the deeper modeled salinities were fresher than observations. Furthermore, the low-salinity surface waters west of the Atchafalaya Bay were confined closer to the shore in the model results than in the observations. It has been suggested (Wiseman et al., 2000) that the turbulence closure schemes used in the model were a primary source of this discrepancy.

Recent improvements have been made to the model under funding from the National Ocean Partnership Program (R. Patchen, personal communication), but output from these model runs were not available for comparison with observations.

2.5 Conclusions

While it is esoterically pleasing to be able to model the shelf circulation and water properties using fully three-dimensional, time-dependent models, it is intriguing that the improvements in hindcast skill associated with today's models over lower dimensional models do not appear to be extreme. The cause of this is unclear, but may be related to the extremely frictional behavior of the water column at weather-band frequencies in this shallow environment, particularly during winter periods. While awaiting the next generation of three-dimensional models, it might be useful to try to understand some of the aspects of the shelf dynamics that can be readily understood using simple models. We have already mentioned the appeal and success of linear, one-dimensional balances between wind stress and bottom friction, e.g. Murray (1998), Walker et al. (2001). In the remainder of this report, we consider three such simple models. The first is a steady-state linear model forced by monthly mean winds. This is meant to approximate the Arrested Topographic Wave approach of Csanady (1978). The second is based on the model of Yankovsky and Chapman (1997), who propose that, in the absence of wind forcing, the structure and offshore extent of a buoyancy-driven coastal current will be controlled by bottom boundary layer processes. The final simple approach to be considered is to explore improvements to the understanding of the nearshore current dynamics by including alongshore pressure gradients.

III. VERTICALLY-INTEGRATED, WIND-DRIVEN MODEL OF VERY LOW-FREQUENCY FLOW

3.1 Introduction

Initially, we had intended to try to compare predictions from the arrested topographic wave model of Csanady (1978) to the observed low frequency current fields. A simpler approach, though, was to compare these current observations to predictions from a vertically-integrated, homogeneous, wind-forced model. There is some rational justification, other than ease of application, for this. Csanady's elegant solution of the steady problem resulted from ignoring the linearized friction associated with cross-shore flow. He made the assumption that this term would always be small and was able to derive a consistent solution to the resulting equations. We treat a slowly varying problem, not a steady one. Observationally, we recognize that, at least for brief periods of a few days duration, cross-shelf flows may be significant and contribute to important bottom friction. How this affects the force balance of the slowly-varying flow field is not immediately evident. By using the full equations, though, we can assess the importance of the various terms in the equations of motion, *a posteriori*.

3.2 Model

The model we used was one developed earlier for estuarine studies (Inoue and Wiseman, 2000; Park, 1998). The model equations are those for conservation of mass and momentum. They are written in Cartesian coordinates in terms of the depth-integrated transport (Leendertse, 1967) as:

$$\frac{\partial U}{\partial t}+\frac{\partial\left(U^2/H\right)}{\partial x}+\frac{\partial(UV/H)}{\partial y}+fV=-gH\frac{\partial\varsigma}{\partial x}-\left(\frac{g}{C^2}\right)\left(\frac{U}{H}\right)\sqrt{\left(\frac{U}{H}\right)^2+\left(\frac{V}{H}\right)^2}+\frac{\tau_x}{\rho}+A\nabla^2U \quad (6)$$

$$\frac{\partial V}{\partial t}+\frac{\partial(UV/H)}{\partial x}+\frac{\partial\left(V^2/H\right)}{\partial y}-fU=-gH\frac{\partial\varsigma}{\partial y}-\left(\frac{g}{C^2}\right)\left(\frac{V}{H}\right)\sqrt{\left(\frac{U}{H}\right)^2+\left(\frac{V}{H}\right)^2}+\frac{\tau_y}{\rho}+A\nabla^2V \quad (7)$$

$$\frac{\partial\varsigma}{\partial t}+\frac{\partial U}{\partial x}+\frac{\partial V}{\partial y}=0 \quad (8)$$

$$U=\int_{-h}^{\varsigma}u\,dz \quad (9)$$

$$V=\int_{-h}^{\varsigma}v\,dz \quad (10)$$

$$H=h+\varsigma \quad (11)$$

Where t represents time, x, y, and z are the coordinates of an orthogonal, right-handed Cartesian system, u and v are the horizontal velocity components in the x and y directions, respectively, ζ is the elevation of the free surface above mean sea level, h is the depth of the water when at rest, f is the Coriolis parameter, which is assumed to be constant, g is the acceleration due to gravity, τ_x and τ_y are the x and y components of the wind stress, respectively, ρ is the density of water, assumed to be constant, A is the horizontal eddy viscosity, assumed to be constant, and C is the depth dependent Chezy coefficient. The Chezy coefficient is represented using Manning's coefficient, n, such that

$$C = \frac{H^{1/6}}{n}. \tag{12}$$

Manning's n was set to a constant value of 0.025.

No normal flow and no-slip boundary conditions are used along the land boundaries. Along the southern and eastern open boundaries, radiation boundary conditions (Camerlengo and O'Brien, 1980) are imposed. These boundaries are along the 26 degree parallel of latitude and the 88 degree meridian of longitude.

The model equations are discretized in a finite-difference formulation on the staggered mesh C grid of Arakawa (Mesinger and Arakawa, 1976). The Grammeltvedt C scheme (Grammeltvedt, 1969), which conserves mass and total energy, is employed. For time integration, the leapfrog scheme is used with an Euler step inserted at regular time intervals to eliminate the computational mode due to the central time differencing. For numerical stability, the frictional terms are lagged in time.

The model bathymetry was based on the ETOP05 data set and interpolated onto a grid size of 2.5 minutes in both the latitudinal and longitudinal directions. The minimal depth was set to 5 m and the maximum depth was set to 500 m in order to satisfy the CFL criterion with a reasonable time step.

Monthly wind speed components for the LATEX experimental period were made available by Texas A&M University (courtesy of Matt Howard). These were interpolated onto the model grid and monthly mean wind stress components were estimated using the formula of Thompson, et al. (1983),

$$\tau_0 = \rho_a C_d(a) a V_0 \tag{13}$$

$$a^2 = |V_0|^2 + 4\sigma^2 \tag{14}$$

where τ_0 is the magnitude of the monthly mean wind stress, V_0 is the magnitude of the monthly mean wind speed, and σ is an estimate of the monthly root mean squared wind speed. In this study, we have assumed that σ is approximately 5 m/s. C_d is estimated from the WAMDI (1988) third generation wave model formulation as

$$C_d(a) = 1.2875 \times 10^{-3}, \text{if } a_{10} < 7.5\,\text{m/s} \tag{15}$$

$$C_d(a) = (0.8 + 0.065\, a_{10}) \times 10^{-3}, \text{if } a_{10} \geq 7.5\,\text{m/s} \tag{16}$$

where a_{10} is the wind speed at 10 m height. The monthly mean wind stress, estimated in this manner, was assigned to the last day of the month and linear interpolation between these values was used to assign a wind stress at any particular time step.

The model was spun up from rest. The horizontal viscosity was set to a constant value of 100 m^2/s everywhere except at those grid points where the water depth was 500 m. At these points, which were closest to the open boundaries, the viscosity was set to a value of 1000 m^2/s in order to damp out small-scale noise generated near the open boundaries.

3.3 Comparison to Observations and Discussion

The output of such a simple model is qualitatively consistent with expectation. Transport velocities are only high over the inner shelf. They are generally downcoast (in the sense of Kelvin wave phase propagation) (Figure 5). This is the direction that would be expected from an examination of the monthly mean wind vectors (Cochrane and Kelly, 1986). Along the Texas coastline, the flow reverses during late spring/early summer in response to the strongly upwelling favorable winds along the south Texas coast at that time of year (Figure 6).

Two-week mean currents from the upper current meters at each mooring were smoothed with a two-point box-car filter to produce thirty-day means. These were compared with the model output. Since the moorings did not lie over model grid-points and some smoothing was applied to the ETOP05 bathymetry, the data was compared with model output at the closest point that exhibited a similar depth to that at the mooring. (This is a technique that produced acceptable results when used to evaluate the Princeton-Dynalysis model in Herring et al., 1999). The magnitude and phase of the complex correlation coefficients are presented in Table 1. Assuming a thirty-day decorrelation time scale, Tchebycheff significance levels were estimated for the correlation coefficients. When the correlation coefficients are significant at or above the 80% level, this is indicated in the table. It is interesting to note that this model, forced solely by low-frequency winds, compares most favorably with observations at the same stations where the models of Current (1996) and Herring et al. (1999) compared well. These latter models were forced, though, by high-frequency winds that included the energetic weather band and, in the case of the Herring et al. model, buoyancy flux.

While the correlations, i.e. the comparisons of the shape of the fluctuating component, were often acceptable, the point by point comparisons were not, e.g. Figures 7 and 8. The observed velocities exhibited much higher peak-to-peak variations that did the model output. Furthermore, the model output was often significantly biased with respect to the observations. One might suggest that the observations represent the surface Ekman layer flow and would be expected to be more energetic than the vertically-averaged flow. Yet, the current meters were frequently about 10 m below the sea surface. Also, for the inshore stations considered and

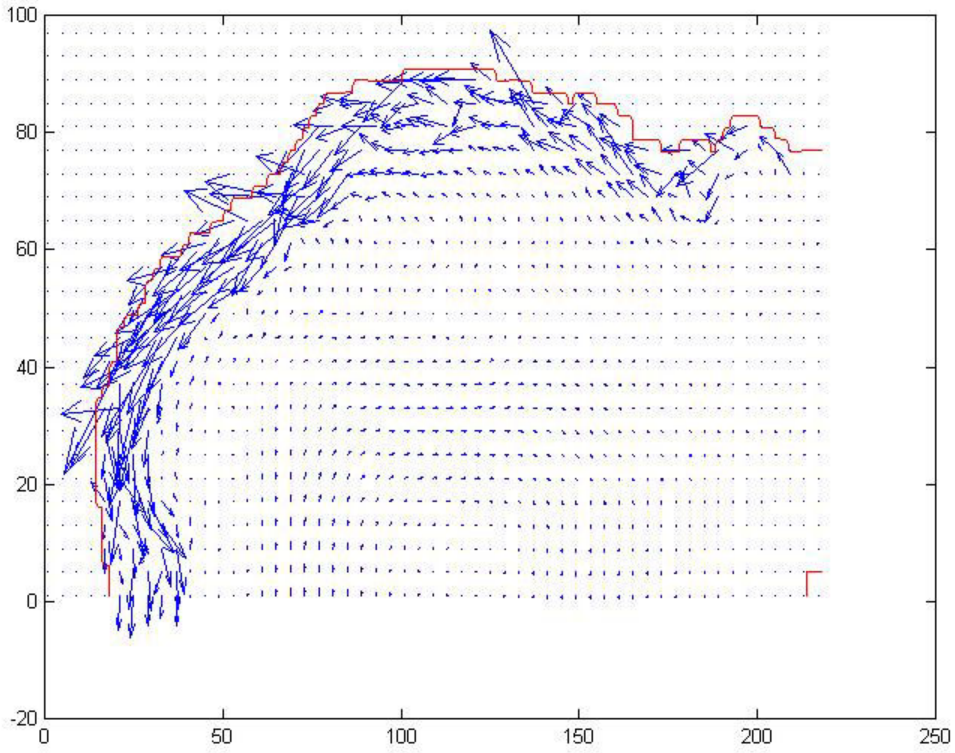

Figure 5. Model output at the end of March 1993. Every fourth velocity vector is printed. The maximum velocity vector shown represents a speed of 14.4 cm/s. The ordinate and abscissa are grid points. Grid point spacing is 2.5 minutes. The origin of the grid points is located at 26^{o} N, 98^{o} W.

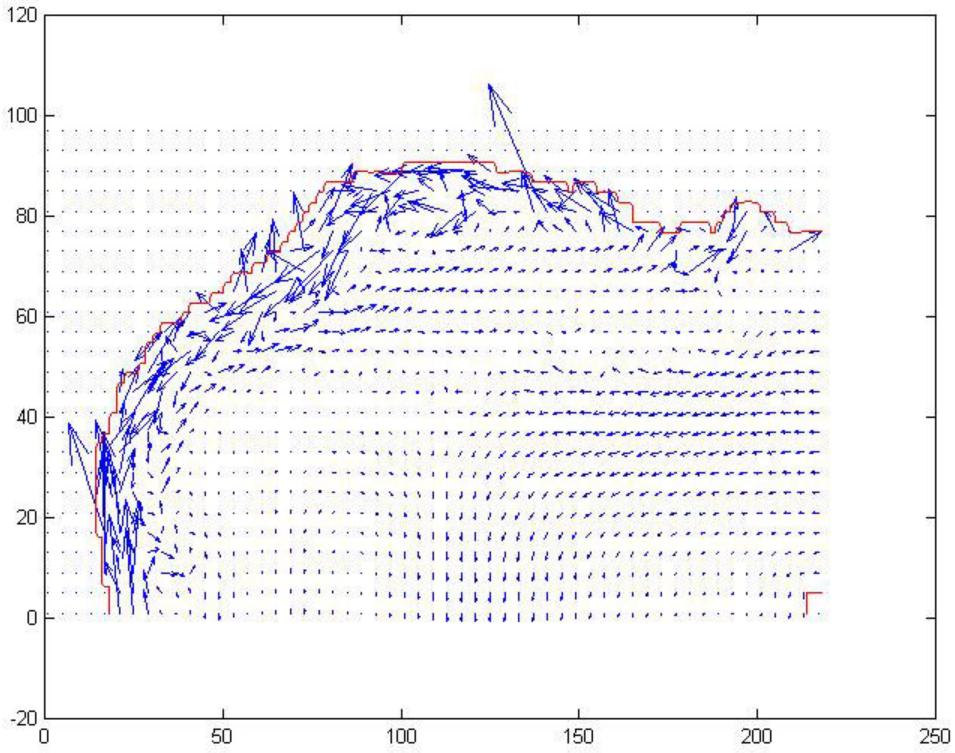

Figure 6. Model output at the end of June 1992. Every fourth velocity vector is printed. The maximum velocity vector shown represents a speed of 9.5 cm/s. The ordinate and abscissa are grid points. Grid point spacing is 2.5 minutes. The origin of the grid points is located at 26^{o} N, 98^{o} W.

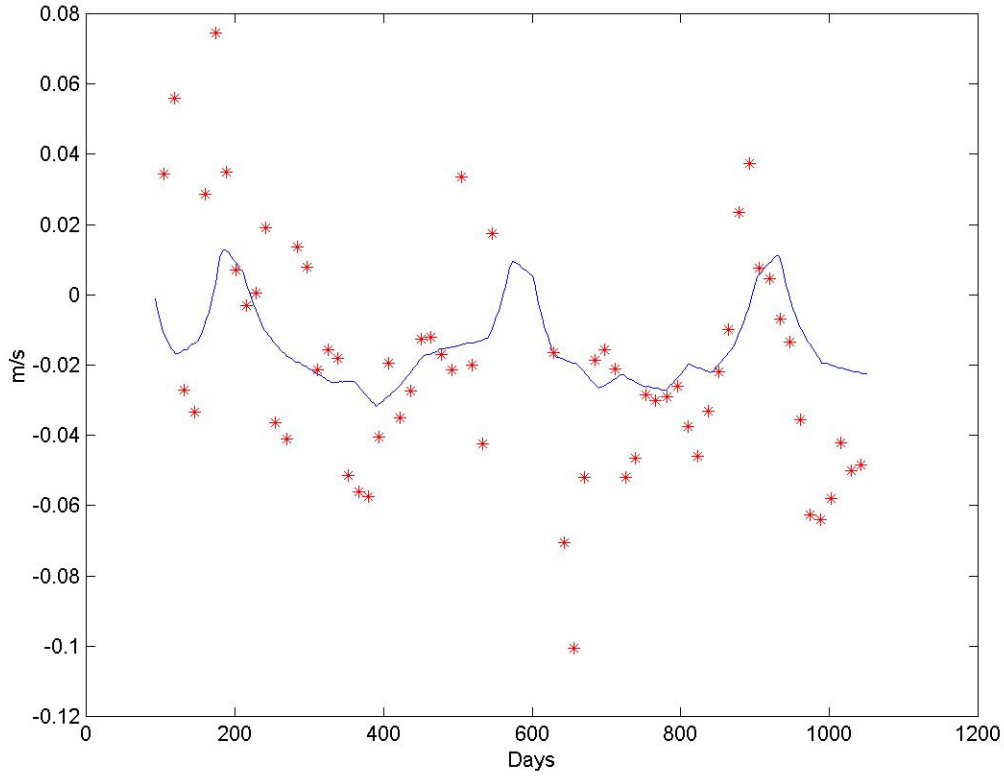

Figure 7. Comparison of the model output eastward velocity (solid line) and monthly mean data (asterisks) plotted at 15-day intervals for LATEX-A station 2 (27.284° N, 96.980° W).

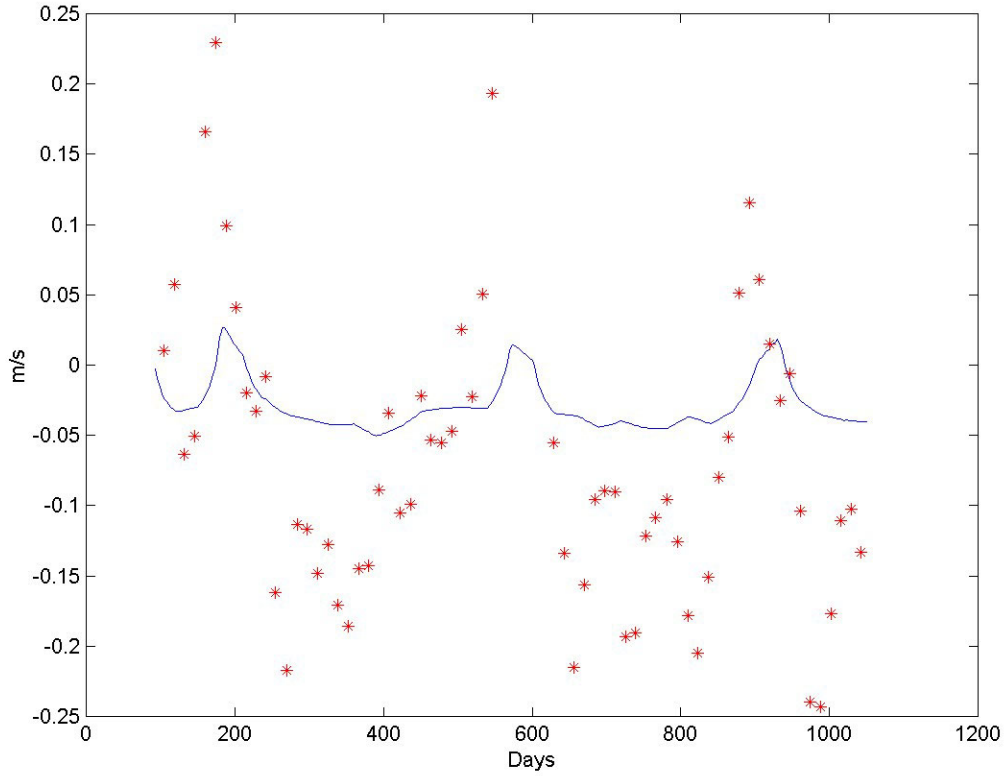

Figure 8. Comparison of the model output northward velocity (solid line) and monthly mean data (asterisks) plotted at 15-day intervals for LATEX-A station 2 (27.284° N, 96.980° W).

Table 1

Complex Correlation Coefficients between Model Output and Observations

LATEX-A Station Number	North Latitude	West Longitude	Mooring Depth (m)	Complex Correlation Coefficient Magnitude	Complex Correlation Coefficient Angle (^{o})
1	27.256	97.246	20	0.60*	1
2	27.284	96.980	37	0.60*	-18
3	27.290	96.736	65	0.38**	6
14	28.395	90.493	47	0.46**	-6
15	28.6608	90.492	27	0.59*	-8
16	28.867	90.491	18	0.19	-5
17	29.196	91.965	8	0.17	-18
18	28.963	91.983	22	0.34	4
19	28.465	92.035	53	0.30	-13
20	29.261	94.064	14	0.15	-17
21	28.837	94.080	24	0.35**	-2
22	28.356	93.956	55	0.30	12
23	28.713	95.536	15	0.65*	-18
24	28.474	95.437	28	0.40**	-11
25	28.162	95.426	37	0.67*	0

* Significant at the 95% level; ** Significant at the 80% level. (Tchebycheff confidence intervals were used. A 30-day decorrelation scale was assumed.)

for those within the 30 m isobath, one would expect the surface and bottom Ekman layers to overlap, at least in a homogeneous fluid. Thus, one is lead to believe that, at least a portion of the discrepancy can be attributed to stratification that was present at the measurement site. The bias between the two signals might also be attributable to a geostrophic flow driven by the slowly-varying ambient stratification.

A comparison of the terms in the model output is revealing. The local accelerations are negligible, as was to be expected from simple scaling arguments, since the time-scale of the forcing is significantly longer than a pendulum day. The lateral dissipation terms are small in comparison to the Coriolis terms. The bottom friction terms, though, are also small. The friction formulation used is, based on prior experience, appropriate for tidal flows and flows in the weather band within the shallow estuaries and nearshore environments of the northwestern Gulf of Mexico. In the model formulation, we accounted for the absence of high frequency components of the wind spectrum in the forcing by enhancing the drag coefficient. Similar arguments have been used to suggest that the bottom drag coefficient should be enhanced in such low frequency models (Current, 1996; discussion in Chuang and Wiseman, 1983). An enhanced bottom drag coefficient, though, would result in a further reduction in the amplitude of the wind-driven flows. We have already noted above that the modeled currents were smaller in amplitude than the observed ones.

The dominant terms in the momentum balance in the model, as presently formulated, are the Coriolis term, the pressure gradient term, and the wind stress term. (In the cross-shore direction, the non-linear term is, on occasion, important, but never makes an order one contribution to the momentum balance.) Although probably unproductive, at this time, it would be intriguing to speculate on the similarities of the balance of forces in this model and those of the steady, central ocean wind-driven flow (Sverdrup, 1947).

Consequently, one is lead to conclude that a simple wind-driven model of the low frequency flows is inadequate. It may capture the qualitative structure and variability of the flows, if the bottom drag coefficient is appropriately tuned. It is unclear whether such tuning merely would be correctly representing bottom frictional processes or would be parameterizing additional processes that are not included in the model formulation, such as baroclinic processes (Chapter IV, this report; Wiseman et al. 1997).

IV. APPLICATION OF THE YANKOVSKY AND CHAPMAN (1997) MODEL

4.1 Introduction

It has been noted above and elsewhere, e.g. Crout et al. (1984), Current (1996), that flows in the wind-driven band are highly coherent with the alongshore wind stress over the Louisiana/Texas inner shelf. At longer periods, there are also indications that wind forcing is a significant contributor to the observed flow variability (Cochrane and Kelly, 1986; Walker et al., 2001; Chapters III and V, this report). At these same longer time scales, baroclinicity has also been implicated as significant to the observed dynamics. Wiseman et al. (1997) have noted that low-passed current shear over the inner shelf near the Texas-Louisiana border is correlated with geostrophic shear. Garvine (2004) has noted similar behavior off the New Jersey coast. It is, thus, reasonable to ask whether the data sets collected during the LATEX-B surveys (Murray, 1998) might contain additional evidence supporting or belying the importance of geostrophy in the dynamics of the Louisiana/Texas inner shelf.

Yankovsky and Chapman (1997) have developed a theory that predicts important length scales associated with a buoyant coastal discharge. They note that, for a bottom-advected discharge, such as is expected to occur offshore and downstream of the Atchafalaya River mouth, the transport eventually would be expected to be confined to the width of the offshore density front, W. If this front is trapped at an equilibrium depth, h_b, then the transport, T_b, is approximately 0.5 $u_z h_b^2 W$, where u_z is the vertical shear of the horizontal flow. (It is assumed that u is zero at the bottom.) The shear, u_z, is given by the thermal wind equations as $g \rho_y/\rho f$, where g is the acceleration due to gravity, ρ is water density, and f is the Coriolis parameter. Substituting for the current shear in the equation defining the transport, one finds $h_b = \sqrt{(2 T_b W \rho f/ g \rho_y)} \approx \sqrt{(2 T_b \rho_0 f/ g \Delta\rho)}$, where ρ_0 is a characteristic density and $\Delta\rho$ is the density difference across the coastal front.

4.2 Comparison to LATEX-B data

The LATEX-B program (Murray, 1998) monitored numerous intensely-sampled CTD sections across the Louisiana Coastal Current perpendicular to the isobaths. These were snap-shots of the hydrographic structure of the current and included effects due to storms and tides. Thus, it may not be expected that the theory developed by Yankovsky and Chapman would be very successful in reproducing observations. The sections did not always sample the offshore edge of the frontal boundary separating the low salinity coastal waters from those of the middle shelf. Nevertheless, they always allowed estimation of the depth at which the coastal front intersected the bottom, h_b. Since the full width of the current was not sampled, the transport within the frontal region could not be unequivocally estimated from the field data. To obtain an estimate of this quantity, we noted the measured discharge of the Atchafalaya River at Simmsport, LA and adjusted this figure upwards to account for offshore waters that had been entrained into the flow to produce the salinity observed inside the front. Finally, we estimated reduced gravity, $g \Delta\rho/\rho_0$, assuming a linear equation of state based solely upon the salinity of the waters. Both these estimates depended upon knowledge of the cross-frontal salinity difference, which was estimated

subjectively from plots of the salinity distribution along the section in question. We estimated h_b, from the observed salinity distributions. We depended heavily upon the salinity distributions because these provided the clearest identification of the frontal structure and its intersection with the bottom. We then compared the observed depth at which the front intersected the bottom with that predicted by the theory of Yankovsky and Chapman (1997). Figure 9 indicates the results of this comparison.

4.3 Critique

In the interests of full disclosure, a few points should be noted. Generally, only data from the first few sections observed downstream of the Atchafalaya River outlet were used in this comparison. The discharge of the Atchafalaya is not steady, while the theory is a steady state theory. It became progressively more difficult to estimate the river discharge appropriate to a given section, and consequently the transport through the section, as the sections were displaced from the mouth of the river. Furthermore, dispersion processes not included in the theory were more likely to have affected the structure of the coastal current the farther downcoast a section was sampled. Finally, it was quickly noted that the comparison broke down, if data from further down the Texas coast were included in the comparison. In some cases, even in the sections retained, a well-defined frontal boundary between the inner shelf, low-salinity waters and the higher salinity, mid-shelf waters was not apparent. In these cases, data from the given section was not utilized in the analyses.

Despite the restricted size of the data set included in this analysis, the theory appears to represent an upper bound on the observed depth of the toe of the front. The clear linear relationship between the predicted and observed parameters when a strong front is present (cross-frontal salinity differences of 7 or higher) is impressive, particularly when one considers the differences between the characteristics under which the observations were collected and those assumed by the theory. The ratio of estimated to observed water depth at the toe of the front is plotted against the cross-frontal salinity difference in Figure 10. It is obvious that the analysis does not produce acceptable estimates of the depth at which the front intersects the bottom when the estimated cross-frontal salinity difference is small. It is unclear, though, whether this results from inabilities of the theory to handle such situations or from difficulties in estimating the inputs to the theory in such weakly stratified situations.

Although the Atchafalaya River discharge is large, its variability is small compared to rivers with a more restricted catchment basin, such as the Eel River (http://ca.water.usgs.gov/archive/waterdata/96/11477000.html). Thus, estimates of the discharge of the Atchafalaya River should be relatively well defined and characteristic of waters that have been recently debouched, since the time scales of discharge variability are long. These estimates should contribute little to the relative error in the estimates of h_b. Estimates of the cross-frontal salinity difference, though, are far less concise and contribute much more to the relative error in h_b. An example of a section exhibiting a very clearly defined salinity front is presented in Figure 11. It should be obvious that, even in such cases of a well-defined front, a certain level of subjectivity and error is incurred in estimation of the various parameters needed to enter into the comparison of observations with theory. In this situation, for example, we have estimated the toe

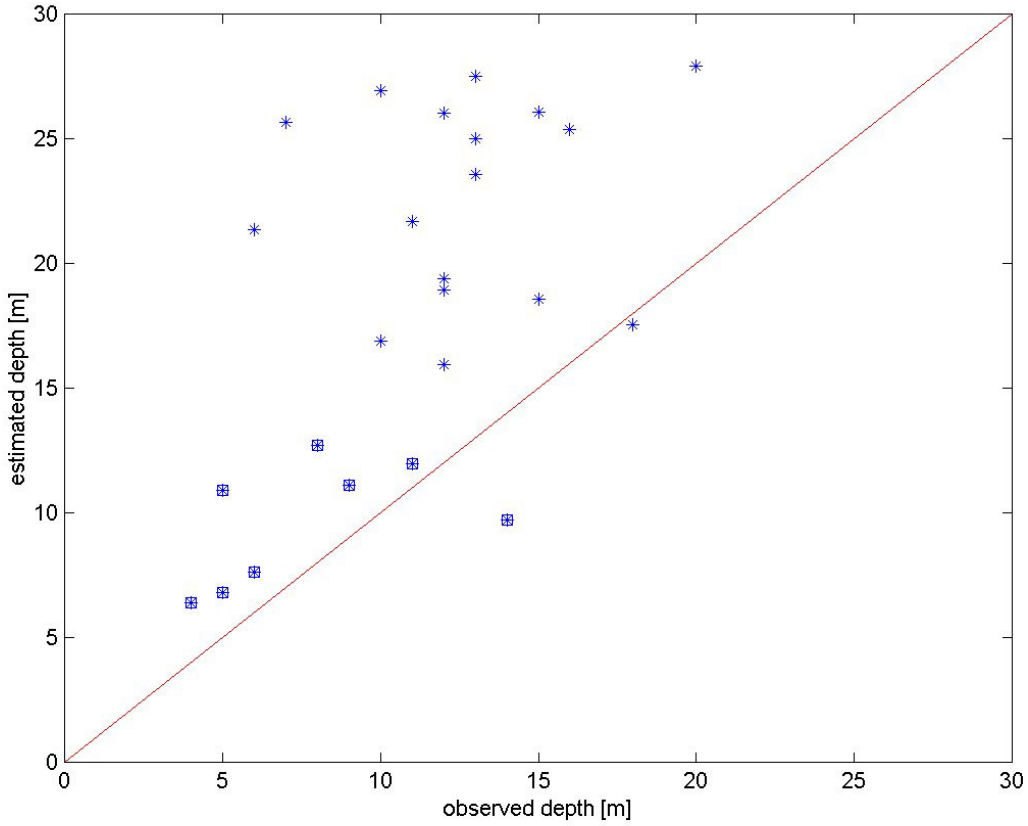

Figure 9. Comparison of the observed depth where the coastal front intersects the bottom with that predicted by the theory of Yankovsky and Chapman (1997) for 25 sections collected during LATEX-B (Murray, 1998). A line with unit slope is overlain on the data. Data points indicated by a square surrounding an asterisk are from sections where the cross-frontal salinity difference is estimated to be at least 7.

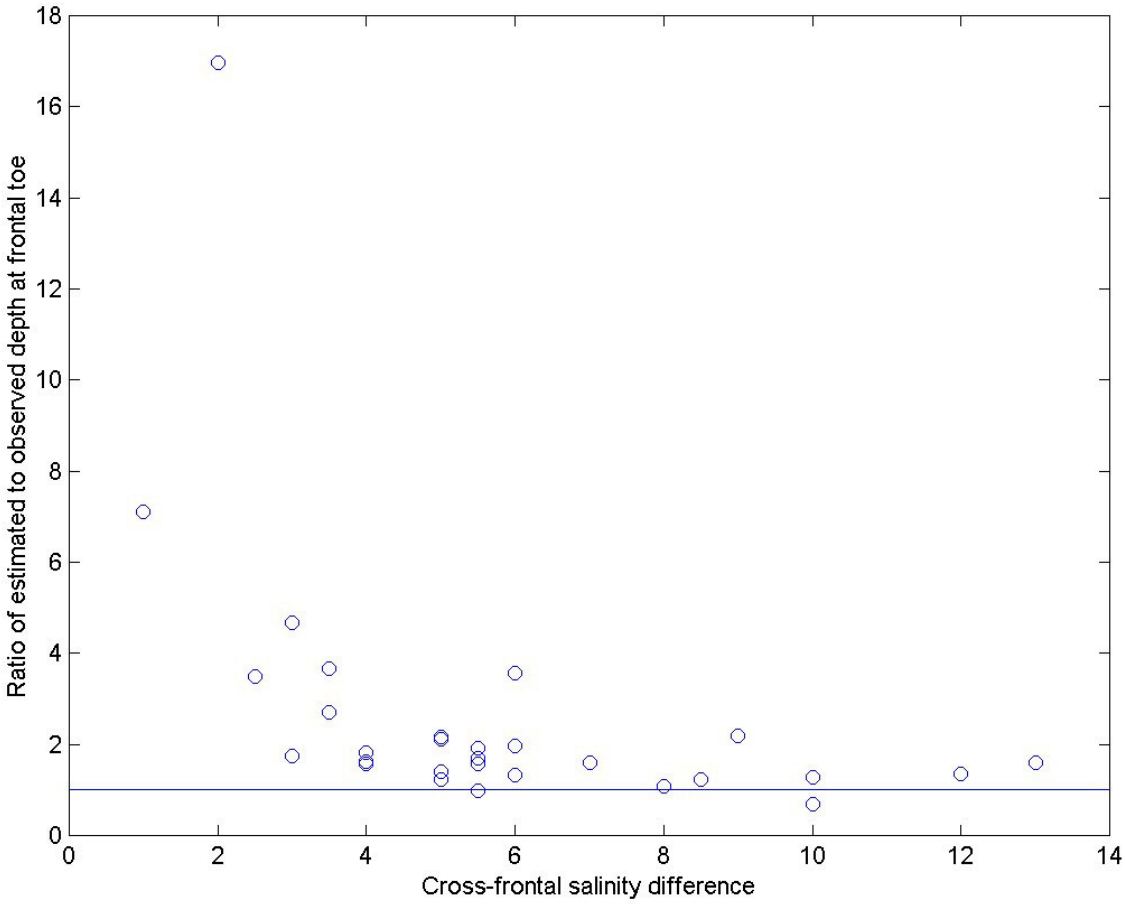

Figure 10. Plot comparing the ratio of water depth at the toe of the salinity front versus the cross-frontal salinity difference for 29 sections west of the Atchafalaya River mouth collected during LATEX-B cruises.

of the front to intersect the bottom at a depth of 12 m, although one could argue coherently for any value between 10 and 14 m. Similarly, we have estimated the cross-frontal salinity difference to be 6 (33 – 27), but slightly different values could also be justified. In situations where the front is less well defined, these estimates become even more imprecise.

While the errors, mentioned above, in estimating input parameters for the comparison are important, they are not the sole cause of discrepancies between the observations and the theory. Dynamical processes occurring at short time scales not accounted for by the theory, particularly wind forcing and non-Fickian dispersion processes, must influence the structure of the front. Perhaps more important is the fact that the theory describes a situation where the system is approaching steady-state. In fact, the model calculations shown in Yankovsky and Chapman (1997) are for a structure that has developed over a 90 day period since river flow was initiated. The sections observed during LATEX-B were probably sampling waters within 10 days of discharge. If the flow structure had not achieved a near steady situation, one might assume that the transport was not fully confined to the frontal region and that transport within the bottom boundary layer was still advecting the observed toe of the front offshore. Indeed, ADCP sections taken during LATEX-B often indicate significant transport inshore of the toe of the front. Such a situation may explain why the theory seems to overestimate the observed depth of intersection between the front and the bottom.

The theory of Yankovsky and Chapman (1997) is based on a simple geostrophic balance in the interior of the flow, which is coupled to a bottom boundary layer. While clearly ignoring many dynamical processes known to be important in the vicinity of the Louisiana Coastal Current, it is intriguing that the theory does as well as it does in predicting the depth at which the coastal salinity front intersects the bottom. This appears to be a clear indication of the dynamical importance of the baroclinic pressure gradients associated with the buoyant discharge from the Mississippi-Atchafalaya system. The data used in this comparison were all collected downcoast of the Atchafalaya River mouth. It remains to be determined how well a similar comparison may describe the coastal current upcoast of the Atchafalaya River mouth, which is associated with the bottom-separated plumes discharged from the Mississippi Delta. The apparent success of the theory at describing structures associated with Atchafalaya River discharge suggest that further development of a robust, time-dependent theory would be beneficial.

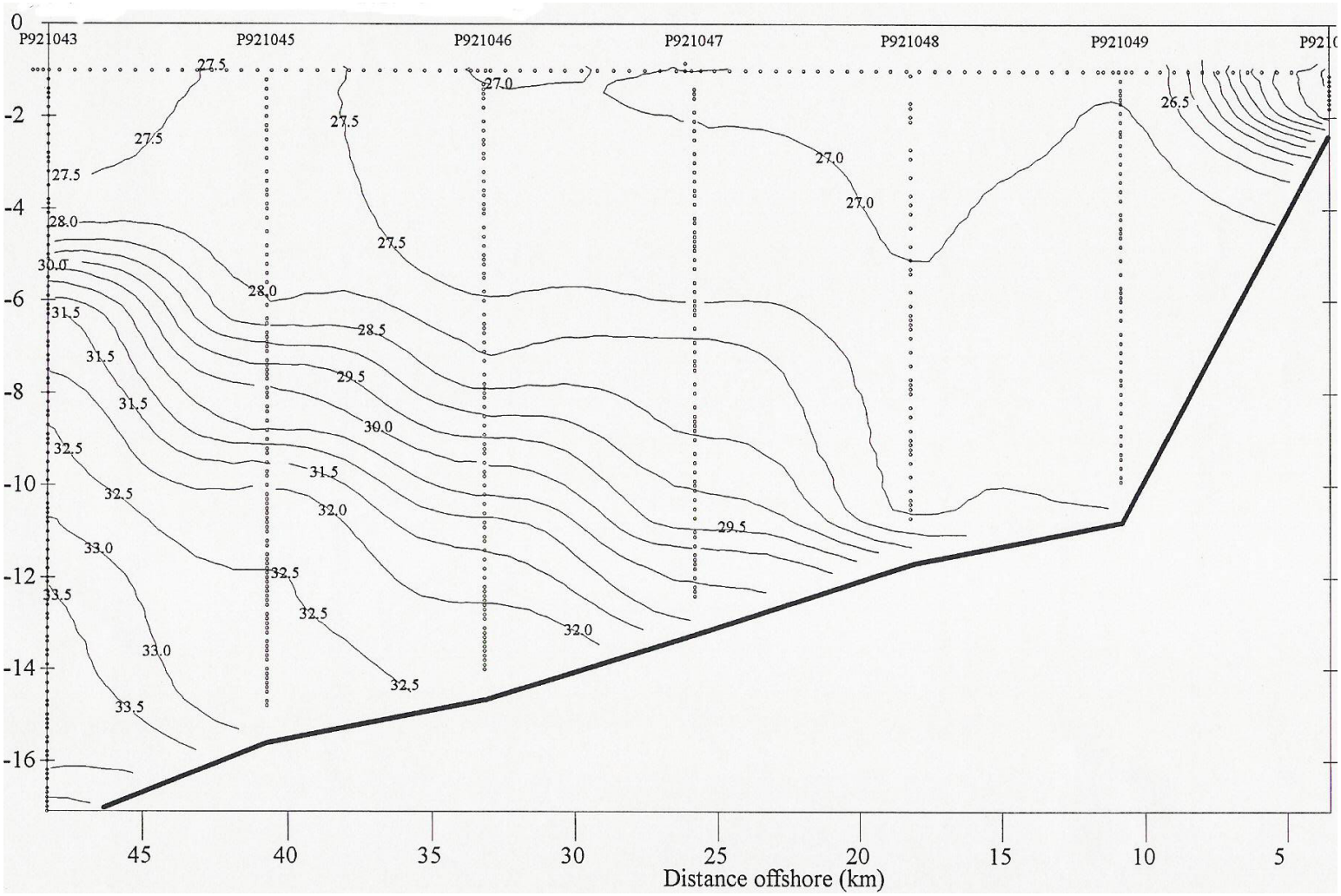

Figure 11. Example of a salinity section across a well-defined coastal front. (The depth scale is in meters.)

V. POSSIBLE IMPORTANCE OF PRESSURE GRADIENTS

5.1 Introduction

As mentioned earlier, longshore pressure gradients have been proposed as a possible mechanism to explain the disparity between the predictions of a local balance between wind stress and bottom (and/or internal) stress and observations. The first person to suggest and estimate the importance of these pressure gradients appears to have been Crout (1983), who followed the formalism of Scott and Csanady (1976). He estimated monthly mean longshore pressure gradient values that were positive in January and March and negative in February and April. He argued that the local frictional balance was more complete in January and March, producing meaningful estimates of the longshore pressure gradients.

Wiseman et al. (1992) analyzed a single month of data and found that only 20% of the pressure gradient variance could be explained by a model including bottom stress, wind stress, and time rate of change of bottom currents in 20 m of water. However, the pressure was strongly coherent with the longshore currents, suggesting cross-shore pressure gradient and longshore currents were coherent. They noted, though, the short duration of the record and its anomalous characteristics when compared to data from other years.

More recently, She (personal communication), has examined a series of long-term, near-surface current records from the east Texas inner shelf and concluded that seasonal geopotential gradients associated with changes in the large scale wind field are important in controlling the regional flow patterns.

5.2 Results from Recent Field Studies

Walker et al. (2001) have analyzed a series of pressure, water level, and current meter records from the LATEX inner shelf region for the period 1994-1998. They suggest that the character of sub-surface pressure changed depending upon the seasonal characteristics of the regional wind field. During the autumn-winter-spring period, when winds were generally downwelling favorable and strong, the pressure signal was coherent with both the longshore and cross-shore winds within the weather band. In contrast, during the summer, when the winds were upwelling favorable along the Texas and west Louisiana coasts, the pressure signal was coherent, at the low end of the weather band, with the longshore winds, but generally incoherent with the cross-shore winds.

They estimate the longshore pressure distribution, but do not mention the reference level used. We assume that the reference is either the record mean at each station, which is then removed, or the mean over a shorter period of time appropriate to concurrent data at all stations. Both methods have potential associated problems. The means derived from the entire data set are not of equal length, i.e. the data sets are gappy. Thus, the means that are removed from the data would be biased. If the means from concurrent data records are used, the means would be computed from very short data sets. (These same problems plague our own data to be described

later in this chapter.) In either case, only the strongest variations would be significant. Fortunately such large gradients do appear in the data. Over periods of a few days, pressure gradients of 30 mb are seen to develop between Padre Island Coast Guard Station and Freeport, Texas. As a cautionary note, though, it should be mentioned that some tide gauges used were situated within passes and bays where local set-up and set-down could affect the data.

A statistical comparison of pressure gradients between Padre Island, Texas and Sabine Pass, Texas and current measurements over the inner shelf offshore of Cameron, Louisiana, though, suggested significant coherence at periods between 5 and 10 days during the summer upwelling-favorable regime and no strongly significant coherence during the downwelling-favorable regime.

From 14 March through 12 November 2002, under another project (Rabalais et al. 2002a), an acoustic Doppler current profiler (ADCP) was deployed twice at a station in 20 meters of water midway between the Mississippi River birdfoot delta and the Atchafalaya River delta (29.5^{o} N 91.25^{o} W) (Figure 12). Ancillary data included bottom mounted pressure cells, roughly at the same isobath, east and west of the mooring and temperature-salinity recorders at the site of the ADCP mooring. Weather data were obtained from a station at Grand Isle (29.27^{o} N 89.96^{o} W).

All data were similarly processed. The semi-diurnal and diurnal tides, as well as the strong inertial oscillations present near 30^{o} N, were eliminated by applying a 101-point, zero-phase filter approximating a flat response out to 40 hours and a linear decay to 27 hour periods (Ormsby, 1961). The resultant low-passed currents and pseudostress were rotated 12^{o} counterclockwise into an alongshore/cross-shore coordinate system.

The expected strong dominance of the alongshore currents was clear in the data. More surprising was the highly variable structure of the flow. Periods of strong vertical shear were interspersed with long periods of very weakly sheared flow. Long periods of flow contrary to the expected westward flow regime were also observed. The vertical density difference between sensors at approximately 7 and 20 m depth showed reduced density difference associated with strong upper layer flow and, consequently, strong shear, even when the river was in flood and the downcoast flow was responsible for a strong lateral buoyancy flux (Figure 13). A significant importance for shear-induced mixing is suggested by these results.

The mean flow is consistent with expectations. The flow is strongly sheared in the alongshore direction. The lower layer flow is weak (Figure 14). The cross shore flow is consistent with a wind-driven downwelling regime as would be expected under the predominantly southeasterly winds affecting the region and a weak indication of reversal is present near bottom.

Both theory and prior isolated observations, led us to anticipate two-layered flows or flow confined to the upper layer, particularly during the highly stratified summer season. Yet, a complex EOF analysis (Kundu and Allen, 1976) indicates that 82% of the variance in the low-passed currents is accounted for by the first mode, which describes nearly unidirectional, vertically-sheared flow (Figure 15). The second EOF mode accounts for only 13% of the variance and describes a two-layered flow field. However, the vertical sigma-t gradient during

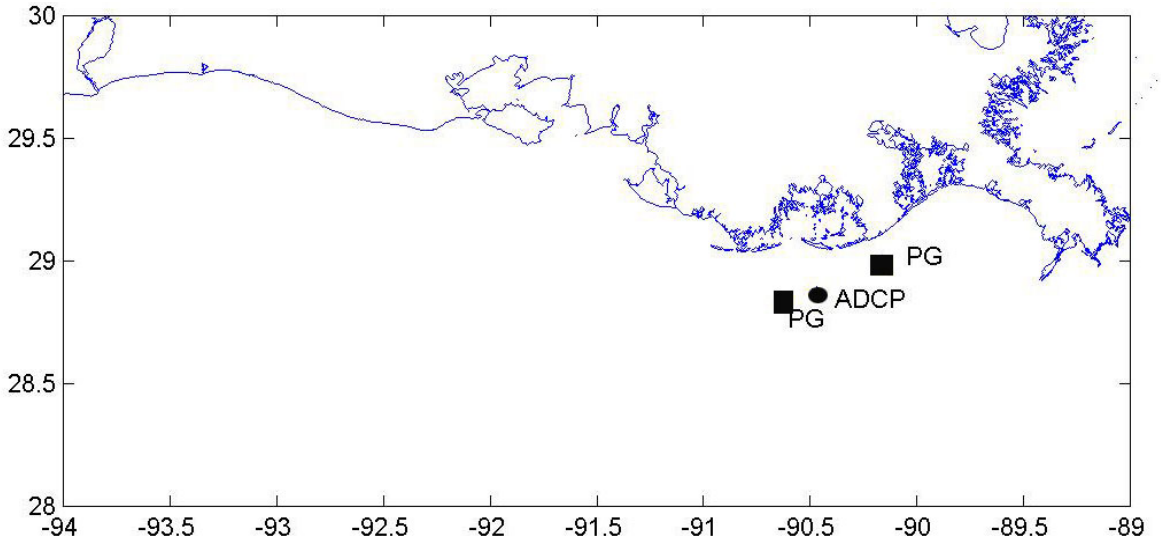

Figure 12. Location map indicating the ADCP and pressure gauge locations. All were deployed at approximately 20 m water depth. (Redrawn from Wiseman et al., 2004.)

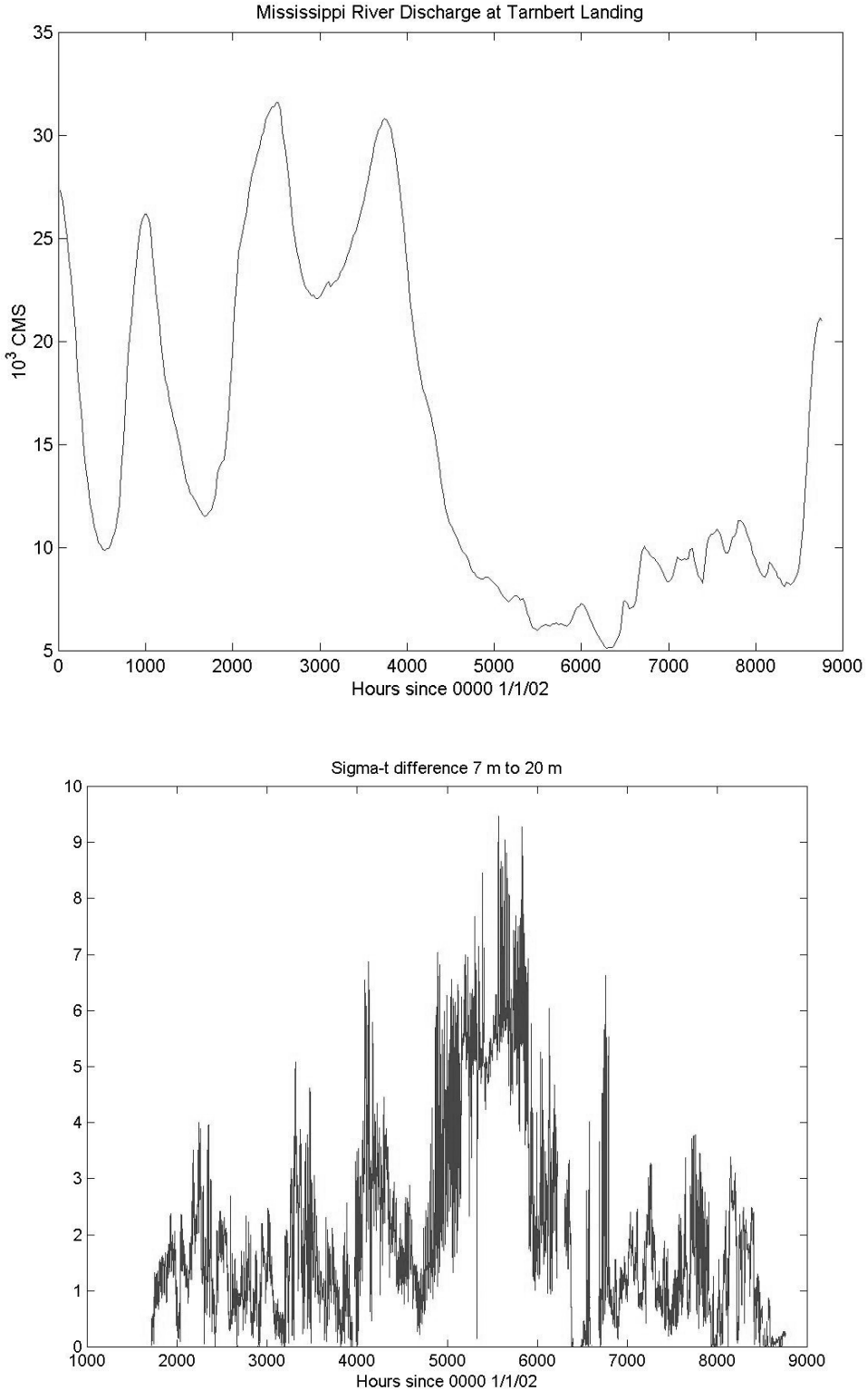

Figure 13. Discharge of the Mississippi River during 2002 (top) and vertical difference between 7 and 20 m depth at the ADCP mooring (bottom). (Redrawn from Wiseman et al., 2004.)

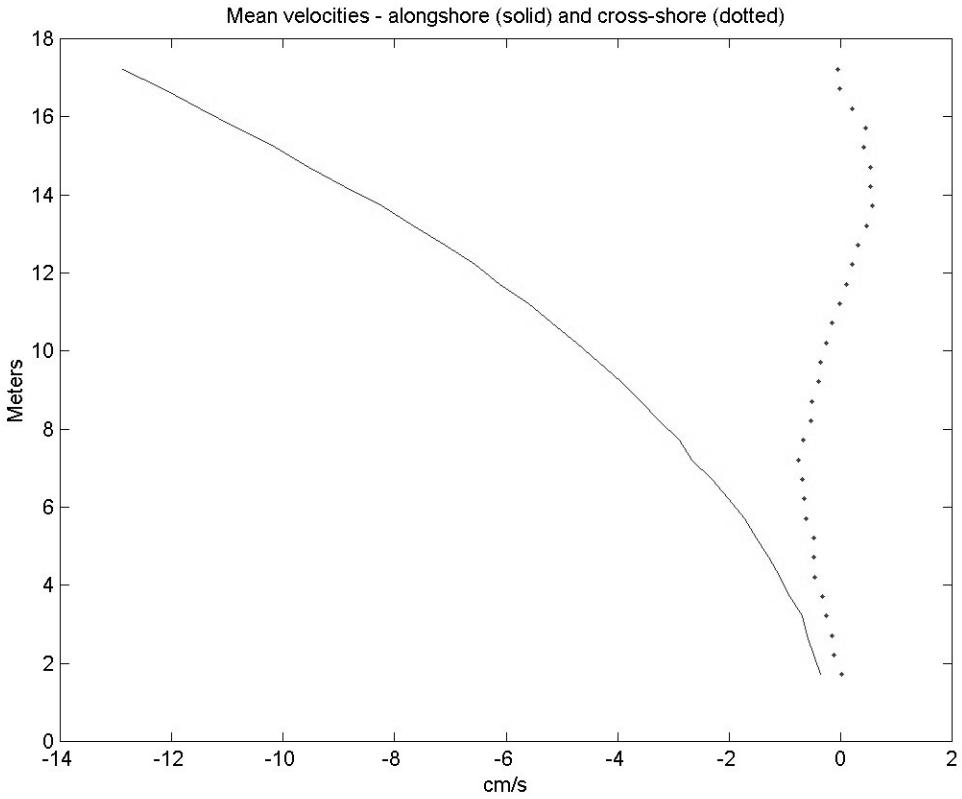

Figure 14. Mean alongshore and cross shore flows during the ADCP deployment (Wiseman et al., 2004).

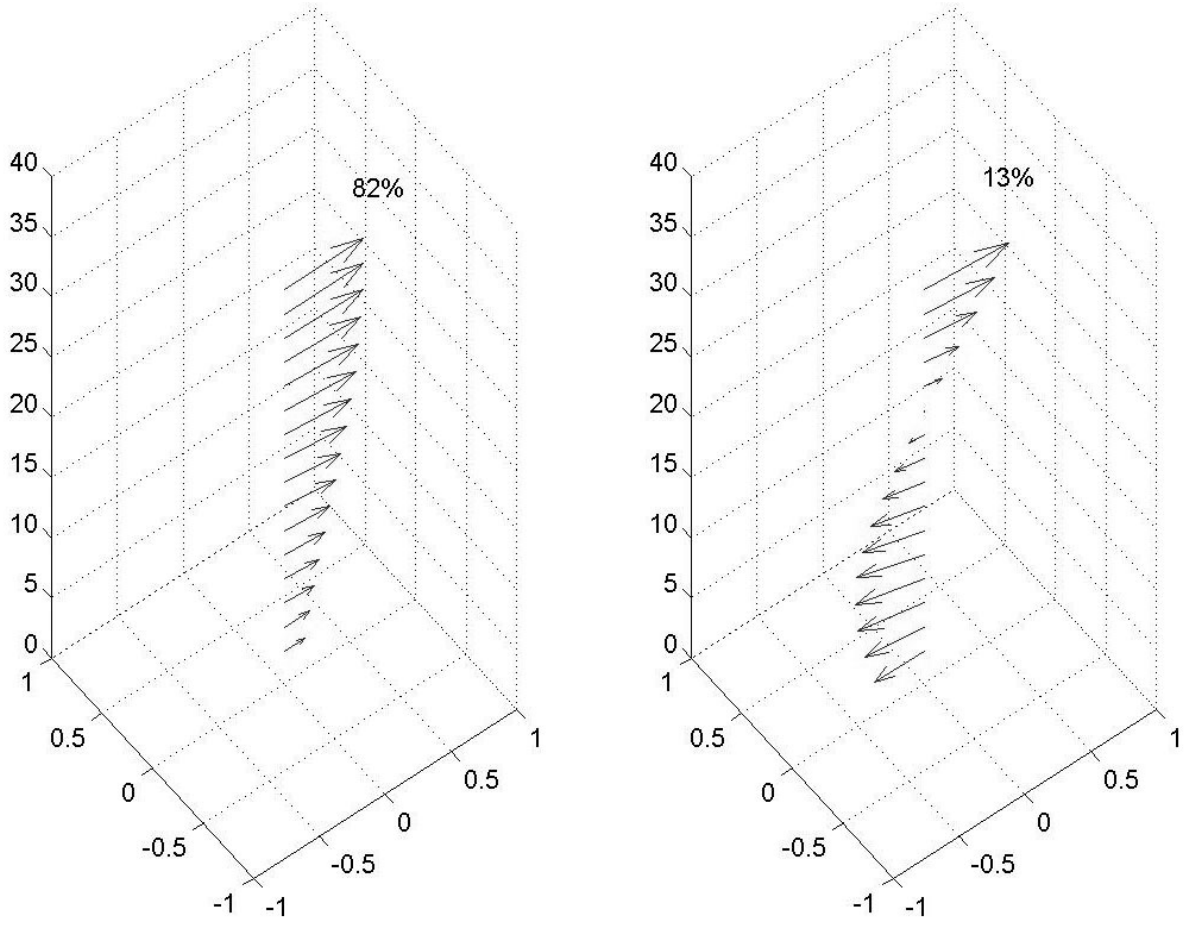

Figure 15. First (left) and second (right) empirical orthogonal functions from the ADCP data. Values associated with every second ADCP bin are plotted (Wiseman et al., 2004).

the analysis period was strong, generally greater than .075 m^{-1} and often 2 or 3 times this (Figure 13).

Such a strong stratification would be expected to isolate the lower layer from direct local wind forcing.

Depth-frequency spectra (not shown) of the alongshore flow indicate significant energy in the diurnal and semi-diurnal tidal-inertial band currents. At the lowest frequencies, intense flows penetrate to the bottom, particularly the alongshore component of flow, while the higher frequency signals suggest surface trapping of the energy. A similar structure is evident in the depth-frequency spectra of the cross shore flows.

The alongshore wind pseudostress is generally coherent with the alongshore currents, at the 95% significance level, below 0.025 cph, except in a narrow band around 0.015 cph (Figure 16). This coherence is slightly stronger at depth than in the upper layers, but it is significant throughout the entire water column. During the first of the two deployments, the upper layer alongshore currents were coherent with the alongshore pressure gradient in bands near 0.01 and 0.02 cph (Figure 17). Similar coherence was observed during the second deployment, but with a more barotropic response, and in a third band of significant coherence near 0.005 cph (Figure 17). It is important to note, though, that two hurricanes passed through the region, approximately a week apart, during the second deployment. The associated signals were very strong in all records and may dominate the cross-spectrum analyses.

5.3 Discussion

These observations raise a number of questions concerning the dynamics of the local flow. What momentum source forces the lower layer flow? Our normal concepts of highly stratified coastal flow as two-layered would preclude local wind forcing of the lower layer. Csanady (1981) suggests that, if the lower layer moves cross-shore as a column in response to the downwelling winds, then Coriolis force acting on this motion will cause an alongshore motion in the correct direction to match observations. This conceptual model, though, assumes two-dimensional and frictionless flow. These assumptions are inconsistent with the real environment. Is lateral advection of alongshore, wind-driven waters associated with the downwelling system sufficiently intense to account for the lower layer observations or are they associated with alongshore pressure gradients? Allen et al. (1995) and Allen and Newberger (1996) have described the flows arising within a two-dimensional model of upwelling and downwelling dynamics and the multiple circulation cells that may result, even without the addition of a coastal buoyancy source. The existing data does not contain the spatial complexity of these models, but the observed cross-shore flows are often multi-layered. Another possibility is that the wind field, interacting with the strong stratification and the crenulated shoreline, produces spatially and temporally varying alongshore pressure gradients that drive the flow in the lower layer. Some evidence for this may be seen in the coherence analyses discussed above, but, without simultaneous cross-shore ADCP records, answers remain largely conjectural. If the lateral flows are important mechanisms for the advection of momentum, how does this affect the oxygen

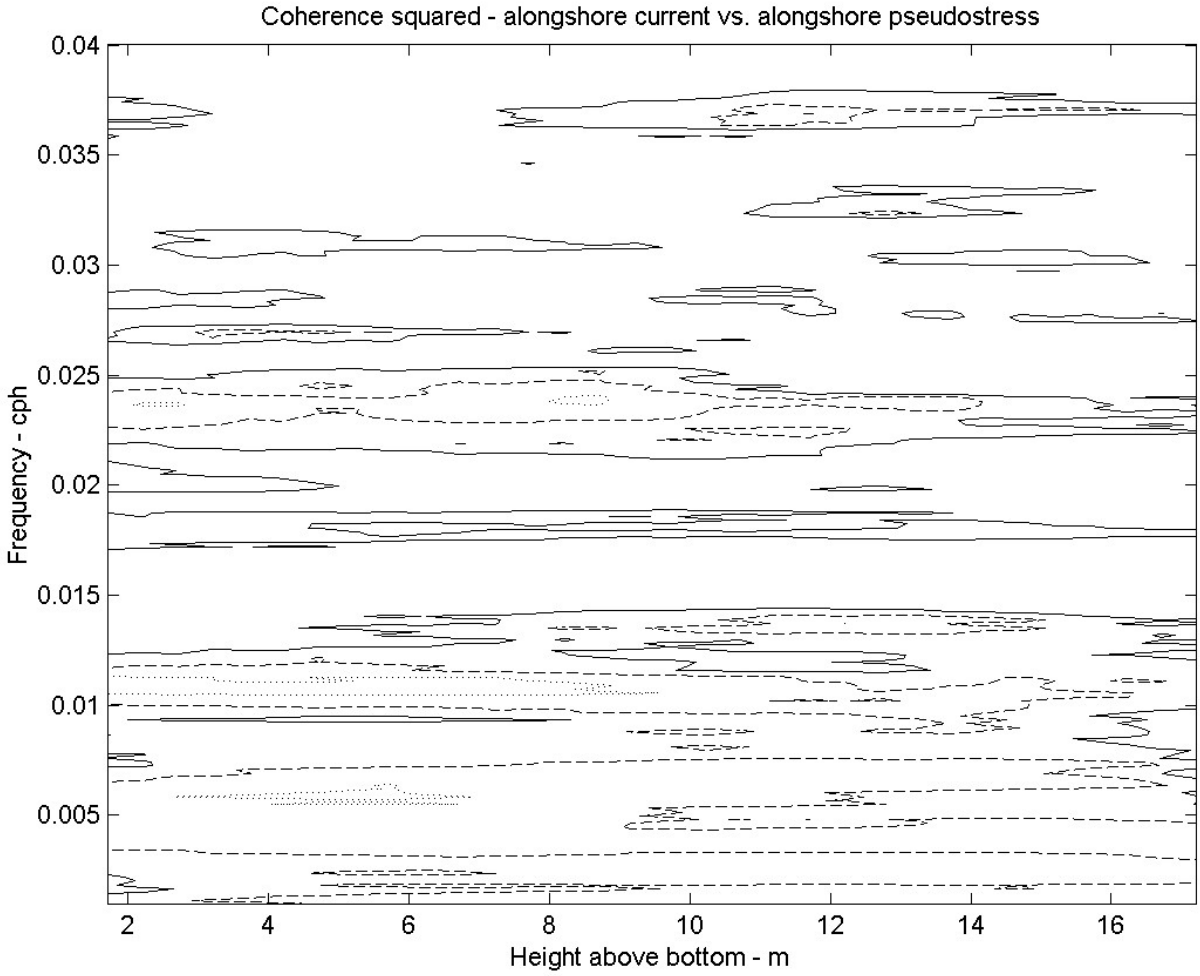

Figure 16. Estimates of coherence squared between alongshore current and alongshore pseudostress. The solid contour is the 95% significance level (0.28), the dashed contour is 0.5, and the dotted contour is 0.75. (Redrawn from Wiseman et al., 2004)

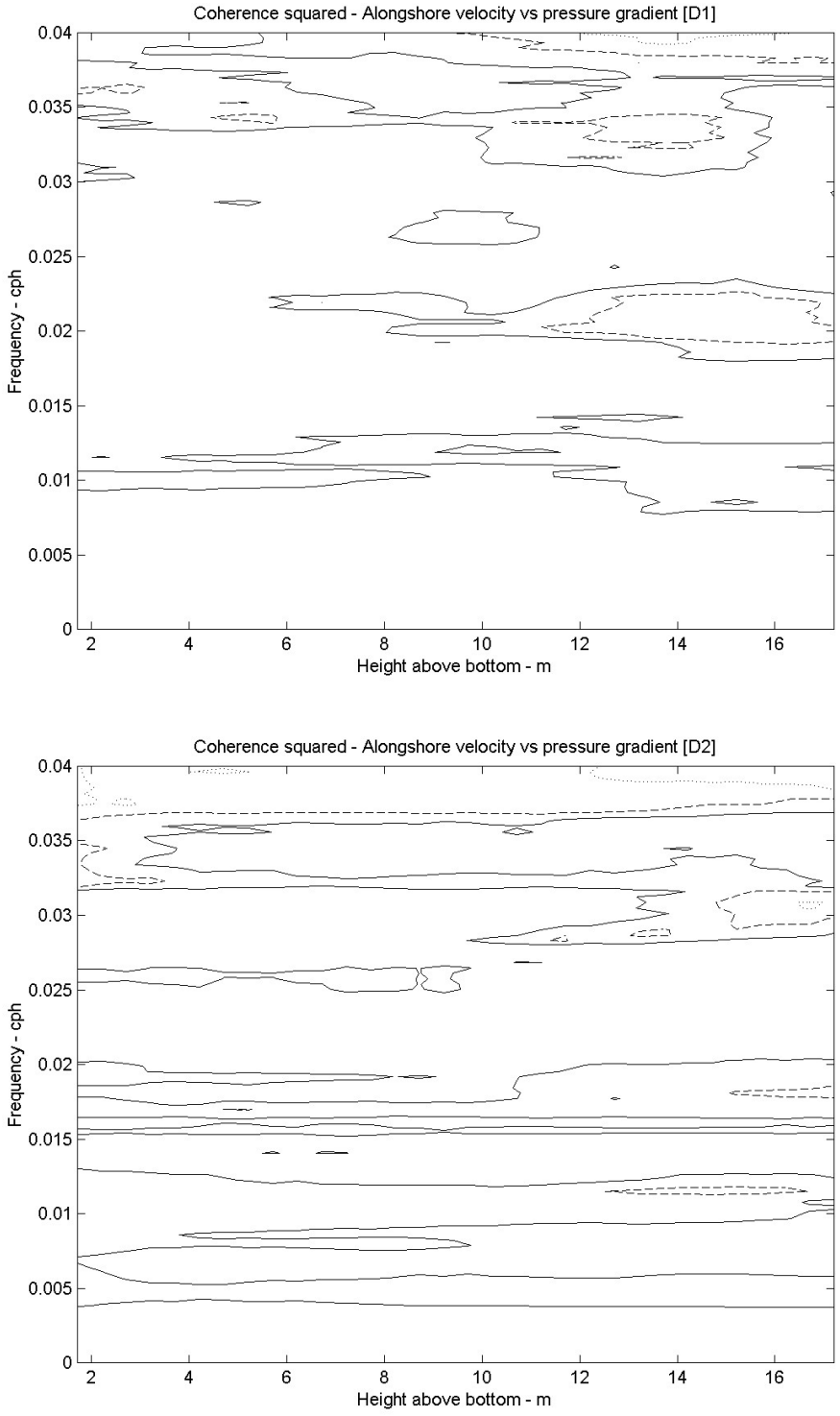

Figure 17. Estimates of coherence squared between alongshore current and alongshore bottom pressure gradient during deployment 1 (top) and alongshore current and alongshore bottom pressure gradient during deployment 2 (bottom). The solid contour is the 95% significance level (0.28), the dashed contour is 0.5, and the dotted contour is 0.75. (Redrawn from Wiseman et al., 2004.)

dynamics? Our near-bottom oxygen records corresponding to the current measurements presented above are still being processed, but historical records (Rabalais et al., 2002b) suggest that near-bottom dissolved oxygen concentrations are modulated at a variety of advective scales, including those associated with upwelling/downwelling cycles.

VI. SUMMARY

We have briefly reviewed the status of existing, reduced dimensionality models of the dynamics of the Louisiana Coastal Current. Many of these are successful at reproducing the qualitative features of the circulation at specific time scales and periods of the year. Local, wind-driven models reproduce credibly the flow variability over the shallow regions of the west Louisiana/east Texas inner shelf, particularly during the winter season, at sub-tidal frequencies within the weather band (Crout et al, 1984; Lewis and Reid, 1985; Walker et al., 2001). Results are noticeably improved when care is taken to accurately account for variability of the bottom dissipation and far-field forcing (Current, 1996). The earlier models were unable to account for alongshore pressure gradients, while that of Current (1996) did. We were, thus, encouraged to assess the importance of such pressure gradients from observations.

The success of such wind-driven models is surprising, since they ignore the riverine buoyancy flux and consequent strong stratification that is characteristic of this region of the Gulf of Mexico. A fully three-dimensional, time-dependent model of the region (Herring et al., 1999) did not perform significantly better at reproducing observations, although it did a good job of capturing the long term mean flows and very low frequency variability. It was also able to reproduce observed stratification moderately well (Wiseman et al., 2000).

In an attempt to discern the plausibility of treating the Louisiana Coastal Current as an arrested topographic wave (Csanady, 1978), we applied an existing vertically-integrated, non-linear numerical model forced by monthly mean wind fields. The results were intriguing but inconclusive. While the momentum balance generally appeared to be in quasi-steady state, i.e. the local accelerations were negligible compared to other forces, **the advective accelerations in the model were, at specific sites, non-negligible**. More interesting was the fact that **the dominant balance of forces in the model was between the Coriolis forces, the surface wind stress, and the pressure gradients**. This may have resulted from not appropriately increasing the bottom drag coefficient to account for motions at frequencies higher than the forcing frequency. Typically, the choice of a constant bottom friction coefficient for subtidal flow modeling is justified by arguing that deterministic tidal currents are much stronger that the subtidal flows being modeled and, thus, dominate the dissipation processes. We selected a friction coefficient that has been used successfully to model tidal flows in the shallow waters of the northwestern Gulf of Mexico. We did not modify the formulation to account for the unresolved tidal flows or the significantly more energetic unresolved weather-band flows. Such modifictions were beyond the scope of this effort, although similar adjustments were made to the wind stress based on the literature. It was also interesting to note that the observations that compared least closely with the model results tended to be the same sites where comparison with prior model results forced by higher frequency winds (Current, 1996; Wiseman et al., 2000) was poor, possibly for many of the same reasons suggested in these references.

Observations of the water depth at which the salinity front, defining the offshore edge of the Louisiana Coastal Current, intersected the bottom were compared with the predictions of a steady-state theory for bottom-trapped, buoyant, coastal discharges (Yankovsky and Chapman, 1997). The comparison was qualitatively successful for the available data. The model appears to predict an upper bound for the intersection depth and the comparison is best when the front is

most clearly developed. **The good comparison of the Yankovsky and Chapman model with observations suggests that further development of a robust, time-dependent theory would be beneficial.**

Recent results by Walker et al. (2001) suggest that inner shelf currents over the west Louisiana shelf are significantly coherent with longshore pressure gradients, during the summer period of upcoast mean flow, at periods between 4 and 10 days. They also suggest weak, but statistically significant, coherence during the downcoast flow regime at periods longer than 10 days. Our comparisons of full water column velocity measurements from a bottom-mounted ADCP and alongshore bottom pressure gradients at a site further east are far less satisfying. **The bottom layer alongshore currents are significantly coherent with the observed alongshore pressure gradients in bands between 25 to 33 hours and near 50 and 100 hours.** The source of the pressure gradient is unclear. We assume that it is dominated by the sea surface slope, but available data is insufficient to rule out a significant contribution from the baroclinic component. The weaker coherence between the upper layer alongshore currents and the alongshore bottom pressure gradient, as well as the weak coherence between the same currents and the alongshore wind stress is disconcerting. This may be due to instabilities in the flow field, which are observed in numerical models (L. Oey, personal communication) and satellite images, but observations are not available with which to verify this conjecture.

There appear to exist situations in time and space along the Louisiana-Texas inner shelf where the bathymetry is sufficiently simple and a single forcing function sufficiently strong that a simplified balance of forces realistically describes the first order dynamics of the coastal current. Such conclusions, though, cannot be generalized to the entire coast or to all time periods. **The Lousiana Coastal Current is a fully three-dimensional, time-dependent system. True understanding of the system will only result from field, theoretical, and numerical simulation studies that account for all four dimensions.**

VII. REFERENCES

Allen, J. S. and P. A. Newberger. 1996. Downwelling circulation on the Oregon continental shelf. Part I: response to idealized forcing. J. Phys. Oceanogr. 26(10):2011-2035.

Allen, J. S., P. A. Newberger, and J. Federiuk. 1995. Upwelling circulation on the Oregon continental shelf. Part I: response to idealized forcing. J. Phys. Oceanogr. 25(8):1843-1866.

Angelovic, J. W. 1977. Environmental studies of the south Texas outer continental shelf, vol. II, physical oceanography. Final Report to Bureau of Land Management, National Marine Fisheries Service, Gulf Fisheries Service, Galveston.

Armstrong, R. 1976. Historical physical oceanography: seasonal cycle of temperature, salinity, and circulation. Environmental assessment of the south Texas outer continental shelf, 1975. NOAA Final Report, Vol. III, Oceanography. 205 pp.

Blumberg, A. F. and G. L. Mellor. 1987. A description of a three-dimensional coastal ocean circulation model. In Heaps, N. ed. Three-Dimensional Coastal Ocean Models. American Geophysical Union. Pp. 1-16.

Camerlengo, A. L. and J. J. O'Brien. 1980. Open boundary conditions in rotating fluids. J. Comp. Phys. 35(1):12-35.

Chen, C., R. O. Reid, and W. D. Nowlin. 1996. Near-inertial oscillations over the Texas-Louisiana shelf. J. of Geophys. Res. 101:3509-3524.

Chen, C., D. Wiesenburg, and L. Xie. 1997. Influences of river discharges on biological production over the inner shelf: a coupled biological and physical model of the Louisiana-Texas shelf. J. Mar. Res. 55:293-320.

Chuang, W. S. and Wm. J. Wiseman, Jr. 1983. Low-frequency current variations west of the Mississippi River Delta. EOS 64, 1021.

Cho, K., R. O. Reid, and W. D. Nowlin, Jr. 1998. Objectively mapped stream function fields on the Texas-Louisiana shelf based on 32 months of moored current meter data. J. Geophys. Res. 103:10,377-10,390.

Cochrane, J. D. and F. J. Kelly. 1986. Low-frequency circulation on the Texas-Louisiana shelf. J. Geophys. Res. 91:10,645-10,659.

Crout, R. L. 1983. Wind-driven, near-bottom currents over the west Louisiana inner shelf. Ph. D. Dissertation, Louisiana State University, Baton Rouge, LA. 117 pp.

Crout, R. L., W. J. Wiseman, Jr., and W. S. Chuang. 1984. Variability of wind-driven currents, west Louisiana inner continental shelf:1978-1979. Contrib. Mar. Sci. 27:1-11.

Csanady, G. T. 1978. The arrested topographic wave. J. Phys. Oceanogr. 8:47-62.

Csanady, G. T. 1981. Circulation in the coastal ocean. Advances in Geophysics 23:101-183.

Current, C. L. 1996. Spectral model simulation of wind driven subinertial circulation on the inner Texas-Louisiana shelf waters of the northern Gulf of Mexico. Unpublished Ph. D. dissertation. Dept. of Oceanography, Texas A&M University, College Station, TX. 159 pp.

Daddio, E., W. J. Wiseman, Jr., and S. P. Murray. 1978. Inertial currents over the inner shelf near 30^{o}N. J. Phys. Oceanogr. 8:728-733.

DiMarco, S. F. and R. O. Reid. 1998. Characterization of the principal tidal current constituents on the Texas-Louisiana shelf. J. Geophys. Res. 103:3093-3110.

DiMego, G. J., L. F. Bosart, and G. W. Endersen. 1976. N examination of the frequency and mean conditions surrounding frontal incursions into the Gulf of Mexico and Caribbean Sea. Mon. Weather Rev. 104:709-718.

Dinnel, S. P. 1988. Circulation and sediment dispersal on the Louisiana-Mississippi-Alabama continental shelf. Unpublished Ph. D. Dissertation, Louisiana State University. Baton Rouge, LA. 173 pp.

Dinnel, S. P. and W. J. Wiseman, Jr. 1986. Fresh water on the Louisiana and Texas shelf. Cont. Shelf Res. 6:765-784.

Dinnel, S. P., W. J. Wiseman, Jr., and L. J. Rouse, Jr. 1997. Coastal currents in the northern Gulf of Mexico. U.S. Dept. of the Interior, Minerals Management Service, Gulf of Mexico OCS Region, New Orleans, La. OCS Study MMS 97-0005. 113 pp.

Frey, H. 1981. Oceanography on the Louisiana inner continental shelf. NOS Strategic Petroleum Reserve Project: Final Report, Vol. I. U.S. Dept. Of Commerce, NOAA, NOS, 343 pp.

Garvine, R. W. 2001. The impact of model configuration in studies of buoyant coastal discharge. J. Mar. Res. 59:193-225.

Garvine, R. W. 2004. The vertical structure and subtidal dynamics of the inner shelf off New Jersey. J. Mar. Res. 62(3):337-371.

Gosselink, J. G., R. R. Miller, M. Hood, and L. Bahr, (eds.) 1976. Environmental baseline study. Louisiana Offshore Oil Port, Inc. New Orleans.

Grammeltvedt, A. 1969. A survey of finite-difference schemes for the primitive equation for a barotropic fluid. Mon. Wea. Rev. 97:384-404.

Gunn, J. T. 1978. Wind-driven transport in 1975, Atlantic coast and Gulf of Mexico. In Ocean Variability Effects on U.S. Marine Fishery Resources 1975. NOAA Tech. Rep. NMFS Circ. 416:229-239.

Gutierrez de Valasco, G. and C. D. Winant. 1996. Seasonal patterns of wind stress and wind stress curl over the Gulf of Mexico. J. Geophys. Res. 101:18,127-18,140.

Hann, R. W. and R. E. Randall. 1981. Evaluation of brine disposal from the Bryan Mound site of the Strategic Petroleum Reserve Program, Final Report, 12-month post-disposal studies, Vol. I. Texas A&M University and Texas A&M Research Foundation.

Herring, J. H., M. Inoue, G. L. Mellor, C. N. K. Mooers, P. P. Niiler, L. -Y. Oey, R. C. Patchen, F. M. Vukovich, and W. J. Wiseman, Jr. 1999. Coastal ocean modeling program for the Gulf of Mexico, Final Report. U.S. Dept. of the Interior, Minerals Management Service, Herndon, VA. Report No. 115. 539 pp.

Hill, G. W., L. E. Garrison, and R. E. Hunter. 1975. Maps showing drift patterns along the north-central Texas coast, 1973-1974. U.S. Geol. Surv. Misc. Field Studies Map MF-714.

Hitchcock, G. L., W. J. Wiseman, Jr., W. C. Boicourt, A. J. Mariano, N. D. Walker, T. A. Nelsen, and E. Ryan. 1997. Property fields in an effluent plume of the Mississippi River. J. Mar. Sys. 12:107-125.

Hirsch, R. M., J. R. Slack, and R. A. Smith. 1982. Techniques of trend analysis for monthly water quality data. Water Resources Research. 18:107-121.

Howard, M. 1996. The spring transition to upcoast flow along the Texas-Louisiana shelf. EOS, Trans. AGU 76:OS97 (supplement).

Huh, O. K., L. J. Rouse, Jr., and N. D. Walker. 1984. Cold air outbreaks over the northwest Florida continental shelf: heat flux processes and hydrographic changes. J. Geophys. Res. 89:717-726.

Inoue, M. and W. J. Wiseman. 2000. Transport, mixing and stirring processes in a Louisiana estuary: a model study. Estuarine, Coastal and Shelf Science 50(4):449-466.

Kimsey, J. B. and R. F. Temple. 1963. Currents on the continental shelf of the northwestern Gulf of Mexico. U.S. Bureau of Commercial Fisheries Circular 161. Pp. 23-27.

Kimsey, J. B. and R. F. Temple. 1964. Currents on the continental shelf of the northwestern Gulf of Mexico. U.S. Bureau of Commercial Fisheries Circular 183. Pp. 25-27.

Kundu, P. K. and J. S. Allen. 1976. Some three-dimensional characteristics of low-frequency current fluctuations near the Oregon coast. J. Phys. Oceanogr. 6(2):181-199.

Leendertse, J. J. 1967. Aspects of a computational model for long-period water wave propagation. Memorandum RM-5294-PR, Rand Corporation, Santa Monica, CA. 165 pp.

Lewis, J. K. and R. O. Reid. 1985. Local wind forcing of a coastal sea at subinertial frequencies. J. Geophys. Res. 83: 466-478.

Li, Y., W. D. Nowlin, Jr., and R. O. Reid. 1997. Mean hydrographic fields and their interannual variability over the Texas-Louisiana continental shelf in spring, summer, and fall. J. Geophys. Res. 102:1027-1049.

Mesinger, F. and A. Arakawa. 1976. Numerical methods used in atmospheric models. GARP Publication Series No. 17, World Meteorological Organization, Geneva, Switzerland. 64 pp.

Murray, S. P. 1998. An observational study of the Mississippi-Atchafalaya coastal plume: Final report. U.S. Dept. of the Interior, Minerals Management Service, Gulf of Mexico OCS Region, New Orleans, LA. OCS Study MMS 98-0040. 513 pp.

Nowlin, W. D., Jr., A. E. Jochens, R. O. Reid, and S. F. DiMarco. 1998. Texas-Louisiana shelf circulation and transport processes study: synthesis report. Volume 1: technical report. U.S. Dept. of the Interior, Minerals Management Serice, Gulf of Mexico OCS Region, New Orleans, LA. OCS Study MMS 98-0035. 502 pp.

Nowlin, W. D. and C. A. Parker. 1974. Effects of a cold-air outbreak on shelf waters of the Gulf of Mexico. J. Phys. Oceanogr. 4:467-486.

Oetking, P., R. Back, R. Watson, and C. Merks. 1973. Hydrography of the nearshore continental shelf of south-central Louisiana. In Offshore Ecology Investigations, Gulf Univ. Res. Cons. 52 pp.

Ormsby, J. F. A. 1961. Design of numerical filters with applications to missile data processing. Journal of the ACM. 8(3):440-466.

Park, D. 1998. A modeling study of Barataria Basin system. Unpublished Masters Essay, Department of Oceanography and Coastal Sciences, Louisiana State University, Baton Rouge, LA. 133 pp.

Pollard, R. and R. C. Millard, Jr. 1970. Comparison between observed and simulated wind-generated inertial oscillations, Deep Sea Res. 17:813-821.

Rabalais, N. N., R. E. Turner, and W. J. Wiseman, Jr. 2002a. Gulf of Mexico hypoxia, a.k.a. "the dead zone." Annual Reviews of Ecology and Systematics 33:235-263.

Rabalais, N. N., R. E. Turner, and D. Scavia. 2002b. Beyond science into policy: Gulf of Mexico hypoxia and Mississippi River nitrogen load. BioScience 52:129-142.

Schideler, G. L. 1979. Regional surface turbidity and hydrographic variability on the south Texas continental shelf. J. Sed. Pet. 49:1195-1208.

Scott, J. T. and G. T. Csanady. 1976. Nearshore currents off Long Island. J. Geophys. Res. 81:5401-5409.

J.Smagorinsky. 1963. General circulation experiments with the primitive equations. Monthly Weather Review 93(3):99.

Smith, N. P. 1975. Seasonal variations in nearshore circulation in the northwestern Gulf of Mexico. Contrib. Mar. Sci. 19:49-65.

Smith, N. P. 1978. Low-frequency reversals of nearshore currents in the northwestern Gulf of Mexico. Contrib. Mar. Sci. 21:103-115.

Sverdrup, H. U. 1947. Wind-driven currents in a baroclinic ocean; with application to the equatorial currents of the eastern Pacific. Proceedings of the National Academy of Sciences, 33:318–326.

Thompson, K. R., R. F. Marsden, and D. G. Wright. 1983. Estimation of low-frequency wind stress fluctuations over the open ocean. J. Phys. Oceanogr. 13:1003-1011.

Veronis, G. and H. Stommel. 1956. The action of variable wind stresses on a stratified ocean. J. Mar. Res. 15(1):43-75.

Walker, N. D., E. Jarosz, and S. P. Murray. 2001. An investigation of pressure and pressure gradients along the Louisiana/Texas inner shelf and their relationships to wind forcing and current variability. U.S. Dept. of the Interior, Minerals Management Service, Gulf of Mexico OCS Region, New Orleans, LA. OCS Study MMS 2001-057. 40 pp.

WAMDI (S. Hasselmann, K. Hasselmann, E. Bauer, P. A. E. M. Janssen, G. J. Komen, L. Bertotti, P. Lionello, A. Guillaume, V. C. Cardone, J. A. Greenwood, M. Reistad, L. Zambresky and J. A. Ewing). 1988. The WAM model - a third generation ocean wave prediction model. J. Phys. Oceanogr. 18:1775-1810.

Wiseman, W. J., Jr. and F. J. Kelly. 1994. Salinity variability within the Louisiana coastal current during the 1982 flood season. Estuaries 17:732-739.

Wiseman, W. J., Jr., S. P. Murray, J. M. Bane, and M. W. Tubman. 1982. Physical environment of the Louisiana Bight. Contributions in Mar. Sci. 25:109-120.

Wiseman, W. J., Jr., J. M. Bane, S. P. Murray, and M. W. Tubman. 1975. Small-scale temperature and salinity structure west of the Mississippi River Delta. In Nihoul, J.C.J., ed. Memoires de la Societe Royale des Sciences de Liege, Belgium. X:277-285.

Wiseman, W. J., Jr., V. J. Bierman, Jr., N. N. Rabalais, and R. E. Turner. 1992. Distribution and characteristics of hypoxia on the Louisiana shelf in 1990 and 1991. Nutrient Enhanced Coastal Ocean Productivity. TAMU-SG-92-109. Texas A&M University Sea Grant College Program, College Station, TX. Pp. 21-26.

Wiseman, W. J., Jr., J. M. Grymes III, and W. W. Schroeder. 1998. Coastal wind stress variability along the northern Gulf of Mexico. In Dronkers, J. and M. Scheffers, eds. Physics of Estuaries and Coastal Seas. Balkema, Rotterdam. Pp. 55-61.

Wiseman, W. J., Jr., M. Inoue, R. Patchen, V. Ransibrahmanakul, S. P. Murray, and S. DiMarco. 2000. Hydrography of the Louisiana coastal current: model-data comparison. In Yanagi, T. ed. Interactions between estuaries, coastal seas, and shelf seas. Terra Scientific Publishing Company (TERRAPUB), Tokyo. Pp. 287-302.

Wiseman, W. J., Jr., N. N. Rabalais, R. E. Turner, S. P. Dinnel, and A. MacNaughton. 1997. Seasonal and interannual variability within the Louisiana coastal current: stratification and hypoxia. J. Mar. Sys. 12:237-248.

Wiseman, W. J., Jr., N. N. Rabalais, R. E. Turner, and D. Justic. 2004. Hypoxia and the physics of the Louisiana coastal current. In Nihoul, J.C.J., P. O. Zavialov, and P. P. Micklin, eds. Dying and Dead Seas Climatic Versus Anthropic Causes. Kluwer. Pp. 359-372.

Yankovsky, A. E. and D. C. Chapman. 1997. A simple theory for the fate of buoyant coastal discharges. J. Phys. Oceanogr. 27:1386-1401.

The Department of the Interior Mission

As the Nation's principal conservation agency, the Department of the Interior has responsibility for most of our nationally owned public lands and natural resources. This includes fostering sound use of our land and water resources; protecting our fish, wildlife, and biological diversity; preserving the environmental and cultural values of our national parks and historical places; and providing for the enjoyment of life through outdoor recreation. The Department assesses our energy and mineral resources and works to ensure that their development is in the best interests of all our people by encouraging stewardship and citizen participation in their care. The Department also has a major responsibility for American Indian reservation communities and for people who live in island territories under U.S. administration.

The Minerals Management Service Mission

As a bureau of the Department of the Interior, the Minerals Management Service's (MMS) primary responsibilities are to manage the mineral resources located on the Nation's Outer Continental Shelf (OCS), collect revenue from the Federal OCS and onshore Federal and Indian lands, and distribute those revenues.

Moreover, in working to meet its responsibilities, the **Offshore Minerals Management Program** administers the OCS competitive leasing program and oversees the safe and environmentally sound exploration and production of our Nation's offshore natural gas, oil and other mineral resources. The MMS **Minerals Revenue Management** meets its responsibilities by ensuring the efficient, timely and accurate collection and disbursement of revenue from mineral leasing and production due to Indian tribes and allottees, States and the U.S. Treasury.

The MMS strives to fulfill its responsibilities through the general guiding principles of: (1) being responsive to the public's concerns and interests by maintaining a dialogue with all potentially affected parties and (2) carrying out its programs with an emphasis on working to enhance the quality of life for all Americans by lending MMS assistance and expertise to economic development and environmental protection.

MMS Securing Ocean Energy & Economic Value for America